agso RESEARCH NEWSLETTER

'Geoscience for Australia's Future'

Number 22 May 1995

Recent NGMA mapping highlights the metallogenic potential of the East Kimberley

During the 1994 field season, AGSO and the Geological Survey of Western Australia (GSWA) completed the second-generation geological mapping of the Gordon Downs and Dixon Range 1:250 000 Sheet areas of the East Kimberley as part of the Kimberley–Arunta National Geoscience Mapping Accord (NGMA) project. The new mapping has resulted in significant changes to the interpreted distribution and stratigraphic relationships of the Proterozoic units, and highlights the potential of this part of the Halls Creek Orogen for diverse styles of gold, base-metal, rare-earth and associated elements, diamonds, platinum-group elements (PGEs), chromium, nickel, copper, titanium, and vanadium occurrences (Fig. 1).

The Gordon Downs and Dixon Range 1:250 000 Sheet areas have afforded considerable interest to mineral exploration companies since the discovery of small lode and alluvial gold deposits near Halls Creek in 1885 — the first discovery of payable gold in Western Australia. In spite of the continued exploration for various metals, and the discovery of a number of prospects, mineral production in the two Sheet areas has been confined to small-scale goldmining. Previously mapped in the early 1960s (Dow & Gemuts 1969: *BMR Bulletin* 106), the two Sheet areas were remapped in 1990–94 with the help of new aeromagnetic and gamma-ray spectrometric data (acquired along lines spaced 400 m apart), Landsat–5 Thematic Mapper imagery, and 1:25 000 colour aerial photographs. AGSO and GSWA will release preliminary 1:100 000 geological maps, complemented by geochemical and geochronological databases and GIS thematic packages, in 1995–96.

Rock types believed to be prospective for various types of precious, base-metal, and rare-earth-element (REE) occurrences define a parallel series of northeasterly trending metallogenic corridors across the western part of the Gordon Downs and Dixon Range Sheet areas (Fig. 1). The corridors are broadly zoned towards the southeast as follows: Ni–Cu–Co → PGEs–Cr–Ni–Cu–Au → Cu–Pb–Zn → a mixed mineralised zone of Au and REE.

Gold

Economic gold occurrences in the Gordon Downs and Dixon Range Sheet areas have been long known to occur close to contacts between the Biscay Formation and overlying Olympio Formation of the Palaeoproterozoic Halls Creek Group, where gold-bearing quartz veins are associated with faults that postdate folding and metamorphism of the host rocks (Dow & Gemuts 1969: *op. cit.*). The new mapping shows that there is also a close spatial relationship between economic gold concentrations and alkaline volcanics in the lower part of the Olympio Formation (Warren 1994: *Australasian Institute of Mining & Metallurgy, Annual Conference Volume*, 117–121); thus, felsic to intermediate alkaline volcanics crop out near the goldmines southeast of Halls Creek (including the Palm Springs project, which will start producing in April 1995), in the Grants Patch area to the northeast, and in the two main areas of current alluvial gold production at Elvire River and Dry Creek (Fig. 1).

Gold and base-metal deposits also occur in hydrothermal quartz breccia veins cutting granite and quartz–feldspar porphyry at the Five Mile Bore and Lady Helen prospects (Pirajno et al. 1994: *Geological Society of Australia, Abstracts 37*, 347) northwest of Halls Creek (Fig. 1).

Copper–lead–zinc

Cu–Pb–Zn occurs at prospects in the Koongie Park and Ilmars–Little Mount Isa areas southwest and northeast, respectively, of Halls Creek (Fig. 1). The Koongie Park prospects are probably of volcanogenic massive sulphide (VMS) type: they are associated with carbonate lenses, banded-iron formation (BIF), and mudstone above a footwall of volcaniclastic rocks and beneath a complex of felsic sills. The NGMA mapping shows that the Koongie Park prospects are hosted by the Koongie Park Formation, dated at 1843 ± 2 Ma (Page et al. 1994: *AGSO Research Newsletter* 20, 5–7), whereas the prospects to the northeast are hosted by the Biscay Formation, dated at ~1880 Ma near the Ilmars prospect (R.W. Page, AGSO, unpublished data).

The VMS model indicates that all the Koongie Park Formation may be prospective for base-metal deposits; the most promising parts are where moderately deep-water depositional environments are

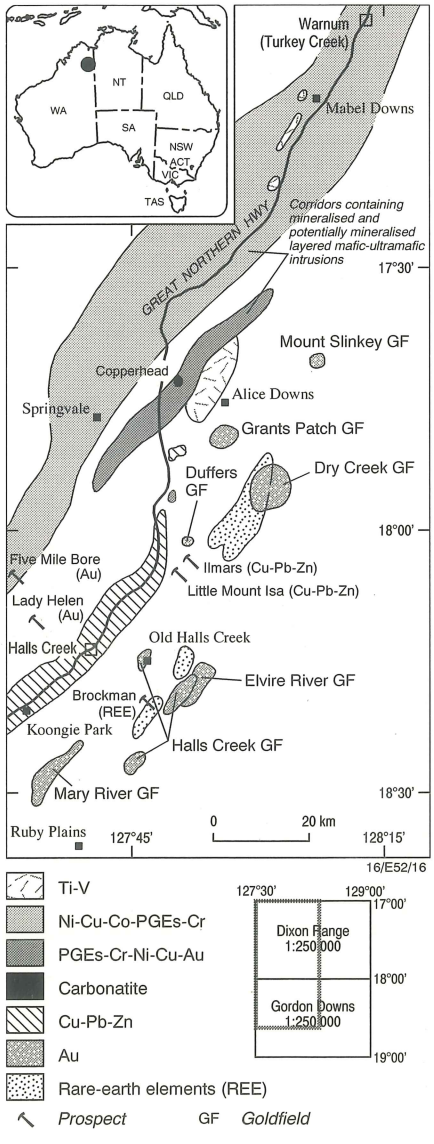

Fig. 1. Distribution of prospective metallogenic corridors, goldfields, and prospects in the western part of the Gordon Downs and Dixon Range 1:250 000 Sheet areas, East Kimberley.

In this issue:

AGSO

Australian Geological Survey Organisation

a research organisation of the Department of Primary Industries & Energy

interpreted. The Ilmars prospect also might be of VMS type; if so, the Biscay Formation would be an additional major exploration target.

Rare-earth elements and associated metals

The currently subeconomic REE and associated metals resource at the Brockman prospect, 17 km southeast of Halls Creek (Chalmers 1990: *Australasian Institute of Mining & Metallurgy, Monograph* 14, 707–709), is hosted by volcaniclastic metasediments associated with alkaline volcanics (Butchers Gully Member) in the lower part of the Olympio Formation. Alkaline volcanics — with high REE and other metal contents and with distinctive gamma-ray spectrometric signatures similar to those at the Brockman prospect — were identified during the NGMA mapping in the Olympio Formation 8 km northeast (e.g., 1.05% REE, 1.8% Zr, 0.25% Nb) and 35 km north-northeast (e.g., 0.6% REE, 1.3% Zr, 0.16% Nb) of the Brockman prospect (Fig. 1). They are potential targets for further exploration of Brockman-type occurrences.

The Copperhead carbonatite–syenite complex (Rugless & Pirajno 1994: *Geological Society of Australia, Abstracts* 37, 385), a newly discovered high-level intrusive plug 200 m wide 12 km northwest of Alice Downs in the McIntosh 1:100 000 Sheet area (Fig. 1), has anomalous REE concentrations, although no potentially economic minerals (apatite, allanite, zircon, pyrochlore, and xenotime) have been identified in it.

Diamonds

Known diamondiferous rocks of the Kimberley region are of two main ages, 1200 and 800 Ma. The older age group includes the world-class Argyle diamond pipe, which represents a high-level crater facies preserved in a downfaulted block just to the north of the Dixon Range Sheet area. Similar high-level bodies might occur beneath Precambrian and Palaeozoic cover sequences in the Dixon Range and Gordon Downs Sheet areas. Other diamond-bearing intrusive bodies known in the Kimberleys have been eroded to the root zone, and are consequently much smaller. Such deposits, though, may be attractive exploration targets if they contain good-quality diamonds at sufficiently high grades.

Platinum-group elements, chromium, nickel, copper, cobalt, and gold

The NGMA mapping has resulted in the subdivision of the Palaeoproterozoic layered mafic–ultramafic intrusions in the East Kimberley into seven major groups on the basis of age of emplacement (U–Pb zircon ages of ~1830–1860 Ma: R. W. Page, AGSO), contact relations with country rocks, degree of fractionation, style of deformation, and types of mineralisation. Details of these groups are summarised by Hoatson & Tyler (1993: *AGSO Research Newsletter* 18, 8–9), Hoatson (1993: *AGSO Research Newsletter* 19, 9–10), and Page et al. (pp. 3–4 herein).

The regional distribution of the mineralised layered intrusions define two northeast-trending corridors crossing the McIntosh, Turkey Creek, and Mount Remarkable 1:100 000 Sheet areas (Fig. 1). Documented and potential mineralisation styles in these intrusions (examples in brackets) include:

- stratiform chromitite layers enriched in PGEs–Ni–Au–Cu immediately below ultramafic–mafic zone contacts (e.g., Panton, Big Ben, West McIntosh, Melon Patch Group);
- stratiform chromitite layers hosted by olivine cumulates either near the base of the ultramafic zones or in the mafic zones (Panton, Big Ben);
- disseminated chromite or sulphides in troctolite and anorthosite in the mafic zones (Springvale, Toby, Dave Hill);
- sulphide-bearing pegmatoidal/porphyritic layers enriched in PGEs–Cu–Ni–Au from 100 m below to 400 m above the contact between the ultramafic and mafic zones;
- structurally controlled hydrothermal–remobilised Cu–Au–Ni–PGEs (?Panton, ?Sally Malay); and
- segregations of Ni–Cu–Co sulphides along the basal contacts beneath the thickest sequence of mafic–ultramafic cumulates (Sally Malay, McKenzies Spring, Norton; see Hoatson: pp. 4–6 herein).

Titanium and vanadium

Fractionated cumulates in the upper levels of layered mafic intrusions in the East Kimberley have potential for concentrations of stratiform titaniferous magnetite and ilmenite with associated vanadium. Thin (centimetre-scale) layers of titaniferous magnetite are hosted by fractionated ferrogabbro and olivine gabbro in the upper part of the large McIntosh intrusion, and thicker layers (up to 5 m) are hosted by magnetite gabbro and leucogabbro in a small mafic intrusion 3 km west of Mabel Downs Homestead (Turkey Creek 1:100 000 Sheet area: AMG coordinates 403282E, 8100095N). Lenses of ilmenite and titaniferous magnetite with 39.4% TiO_2 and 0.99% V have been documented in ferrogabbro of the Frog Hollow mafic intrusion (Hoatson: pp. 4–6 herein), and in gabbro 2 km southeast of the Sally Malay intrusion (Turkey Creek 1:100 000 Sheet area: AMG coordinates 397260E, 8080200N).

Miscellaneous

Thin BIF units are associated with mafic–felsic volcanics and chemical sediments in the Koongie Park Formation near Halls Creek, and in the Biscay Formation to the east, in the Halls Creek 1:100 000 Sheet area. The largest BIF found to date is an elongate body about 1200 m long and 650 m wide in the McIntosh 1:100 000 Sheet area (Hoatson: pp. 4–6 herein). Though not apparently prospective for Fe, some of the BIFs and/or their associated rocks may have potential for precious and base metals (e.g., Au, PGEs, Cu, Pb, Zn).

For further information contact, Drs Dean Hoatson, David Blake, or Gladys Warren (Division of Regional Geology & Minerals, AGSO); Ms Karen Orth (Centre for Ore Deposit and Exploration Studies, Tasmania); or Dr Ian Tyler (GSWA, Perth).

Ocean outfall discharges of nutrients, offshore Sydney

During April 1994, AGSO collaborated with the Victorian Fisheries Research Institute, Department of Conservation & Natural Resources, to study elements of the marine environment in southeast Australia. Aboard RV *Rig Seismic*, they acquired sea-water-nutrient, hydrocarbon, and hydrographic data continuously between the Yarra River (Port Phillip Bay, Melbourne) and Port Jackson (Sydney). These high-resolution data were obtained with the continuous geochemical tracer (CGT) instrumentation, previously used to trace the dispersion of sewage hydrocarbons off Sydney (*AGSO Research Newsletter*, 16, 23–24). Sea water was also sampled in transit for later analysis of heavy metals, particulates, and organic toxicants.

One of the objectives of the work off Sydney was to determine the nature and extent of nutrient discharge to the sea from ocean outfalls. Excessive nutrient loadings may, in some instances, lead to the stimulation of nuisance and toxic algal growth or perhaps eutrophication of local receiving bodies of water. The CGT towfish was set at a depth of about 50 m (where the sewage plume was earlier identified in the water column), and towed directly over the ocean outfalls at Malabar and North Head. Selected data for the Malabar and North Head ocean outfalls are shown in Figures 2 and 3 respectively.

The plume from the outfalls was identified by prominent methane, ammonium, and phosphate anomalies. Ammonium and phosphate anomalies were about ten times the background concentrations at the North Head outfall, and about five times typical background levels over the Malabar ocean outfall. Silicate and nitrate anomalies were also found over both outfalls. The anomalies were estimated to extend over distances of 6–10 km, and concentrations abruptly decreased away from the outfalls. Even though this pilot survey was not intended to map the extent of nutrient dispersion in any detailed way, it did show that the CGT technique is capable of obtaining large amounts of data to map a variety of measured parameters in a way which is superior to traditional fixed-station strategies.

While trapped beneath the thermocline during summer months, when the water column is stratified as a result of surface-water warming, the high concentrations at depth suggest that ammonium, phosphate, and other nutrients leak into the surface water (with lower nutrient concentrations than those at depth), probably by turbulent vertical mixing processes. This anthropogenic source of nutrients to the surface may lead to a stimulation of phytoplankton primary production above typical or historical background levels (Fig. 4a). During the winter months, and storm events in any season, when stratification in the water column is eroded, and the sewage plume may rise to the surface, significant injections of these high nutrient concentrations would accom-

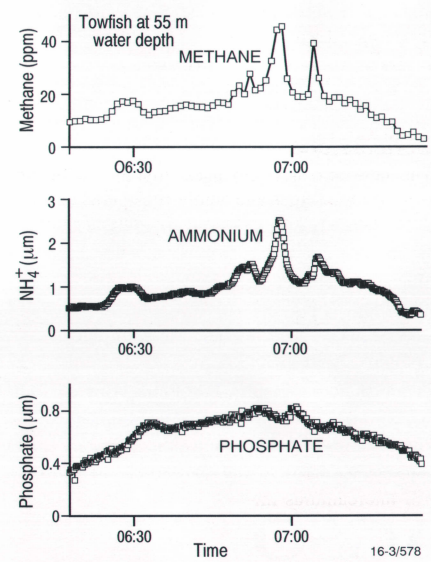

Fig. 2. Methane, ammonium, and phosphate anomalies detected with the CGT apparatus over the Malabar outfall.

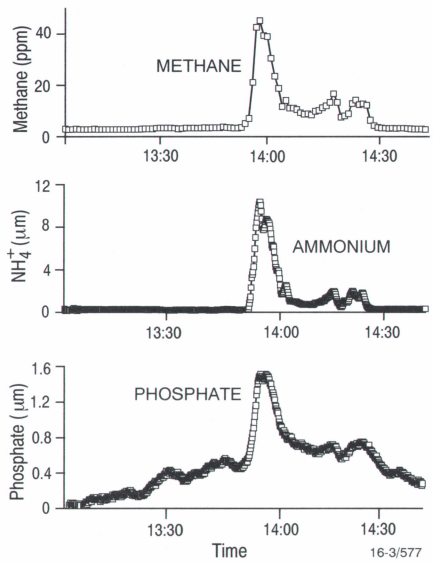

Fig. 3. Methane, ammonium, and phosphate anomalies detected with the CGT apparatus over the North Head outfall.

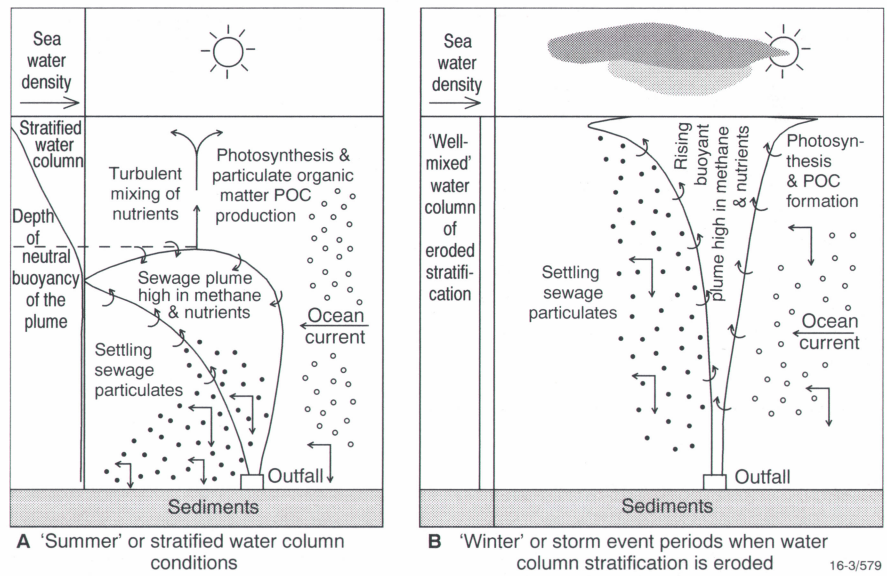

Fig. 4. Schematic representations of mechanisms of nutrient injections into surface oceanic water from the ocean outfalls.

pany the vertical advection of the plume into the surface water. These processes may also result in the stimulation of phytoplankton primary production locally in the nearshore zone. These types of injections of high levels of nutrients into the surface water are probably episodic events, driven by the combined effects of plume buoyancy and erosion of the local water-column stratification by wind mixing and thermohaline convection (Fig. 4b).

Both vertical advective and turbulent mixing processes support a continuous input — albeit at different rates — of anthropogenically sourced nutrients from the ocean outfalls, and high concentrations at depth, into surface waters. These inputs may result in the addition of particulate marine organic matter (as distinct from particulate sewage matter added directly via the outfalls) to the coastal zone. The new data presented here provide new insights into the variety of complex processes operating in the vicinity of the ocean outfalls. This work is important for elucidating the key processes from which environmental monitoring and management strategies can be developed. Implicit in these data are important controls on the potential storage of anthropogenically sourced nutrients in the coastal zone, which have implications for the management of long-term water quality off Sydney.

For more information, contact Dr David Heggie (Division of Environmental Geoscience & Groundwater) at AGSO.

Applications of the laser Raman microprobe to the study of layered intrusions

Raman spectroscopy is a non-destructive technique that can be used for the identification and crystallographic analysis of both transparent and opaque minerals as small as 1–2 μm in diameter. The technique has advantages over analyses by other techniques such as X-ray diffraction and electron microprobe, because little sample preparation is required and samples ranging from hand specimens through polished blocks to thin sections can be rapidly analysed. These features make this an ideal technique for the identification and investigation of the various minerals associated with layered mafic–ultramafic intrusions such as the Archaean Munni Munni Complex, in the west Pilbara Block (WA).

The Munni Munni Complex

The Munni Munni Complex is one of the largest and economically most significant layered mafic–ultramafic intrusions in Australia. Its geology, petrography, geochemistry, and mineralisation have been previously discussed in detail (Hoatson et al. 1992: *Australian Geological Survey Organisation, Bulletin* 242; Barnes & Hoatson 1994: *Journal of Petrology,* 35, 715–751).

The complex can be broadly divided into a lower ultramafic zone and an overlying gabbroic zone on the basis of the distribution of cumulus and intercumulus minerals. The ultramafic zone is largely characterised by varying proportions of cumulus clinopyroxene, cumulus olivine, and intercumulus orthopyroxene; plagioclase, as an intercumulus phase, is restricted to the marginal rocks and the upper 50 m of the ultramafic zone. The base of the gabbroic zone (1850 m level) is defined by the first appearance of cumulus plagioclase, which is associated with cumulus clinopyroxene and cumulus inverted pigeonite. Platinum-group minerals (PGMs) are associated with sulphides in the upper part of a porphyritic plagioclase websterite layer immediately below the ultramafic–gabbroic zone contact (Hoatson & England 1986: *BMR Research Newsletter*, 5, 1–2).

Pyroxenes

The Munni Munni Ca-rich and Ca-poor pyroxenes display fractionation trends that are generally similar to those that characterise large differentiated mafic–ultramafic intrusions of tholeiitic affinity. The Ca-rich pyroxenes display a similar decrease in Ca with fractionation to those of the Skaergaard and Bushveld intrusions, in which Fe replaces Ca and Mg in almost equal proportions. However, the most subcalcic Munni Munni clinopyroxenes are more Fe-rich than the Sudbury, Jimberlana, and Skaergaard clinopyroxenes, and are similar in composition to those of the subcalcic Bushveld clinopyroxenes. The Ca-poor pyroxene trend of the Munni Munni Complex is defined by a continuous evolution with increasing stratigraphic height from bronzite to hypersthene to intermediate pigeonite.

Raman spectra of Munni Munni orthopyroxene and inverted pigeonite with compositions ranging from mg_{54} to mg_{87} (where *mg* equals atomic 100Mg/[Mg + total Fe]) show a systematic increase in the frequency of the Raman bands with increasing *mg* number (Fig. 5). These results show that (at least in binary systems) Raman spectroscopy can be used to obtain semiquantitative chemical analyses owing to the direct relationship between crystal chemistry and crystal structure. Furthermore, it can be used to detect cation order/disorder, and possibly non-stoichiometry too.

Plagioclase

A similar simple shift in Raman frequency with increasing Ca^{2+} content of plagioclase feldspars does not occur, because the low-temperature plagioclase series is not continuous but contains four structural divisions: albites (An_0 to An_3), peristerites (An_3 to An_{22}), intermediate structures (An_{22} to An_{73}), and anorthite structures (An_{73} to An_{100}). Even so, it is still possible to discriminate between the various feldspars because each Raman spectrum produces a unique fingerprint (Mernagh 1991: *Journal of Raman Spectroscopy*, 22, 453–457) with different bands at slightly different frequencies (Fig. 6).

Sulphides

Sulphide-saturated chilled margins occur in the Munni Munni Complex, and are also common in many major layered intrusions elsewhere (e.g., Bushveld, Sudbury, Stillwater, and Duluth). The identification of even microscopic amounts of sulphides in layered intrusions is important, as the timing of sulphur saturation is critical: if a host magma attains sulphur saturation too early in its evolution, any chalcophile metals (e.g., Cu, Ni, and PGEs) will be rapidly depleted in the melt, and cannot be concentrated into mineralised horizons. Sulphide grains of only a few micrometres can be difficult to identify with techniques such as the electron or proton microprobe, because the beam may penetrate into adjoining or underlying sulphide or silicate phases. The very small pene-

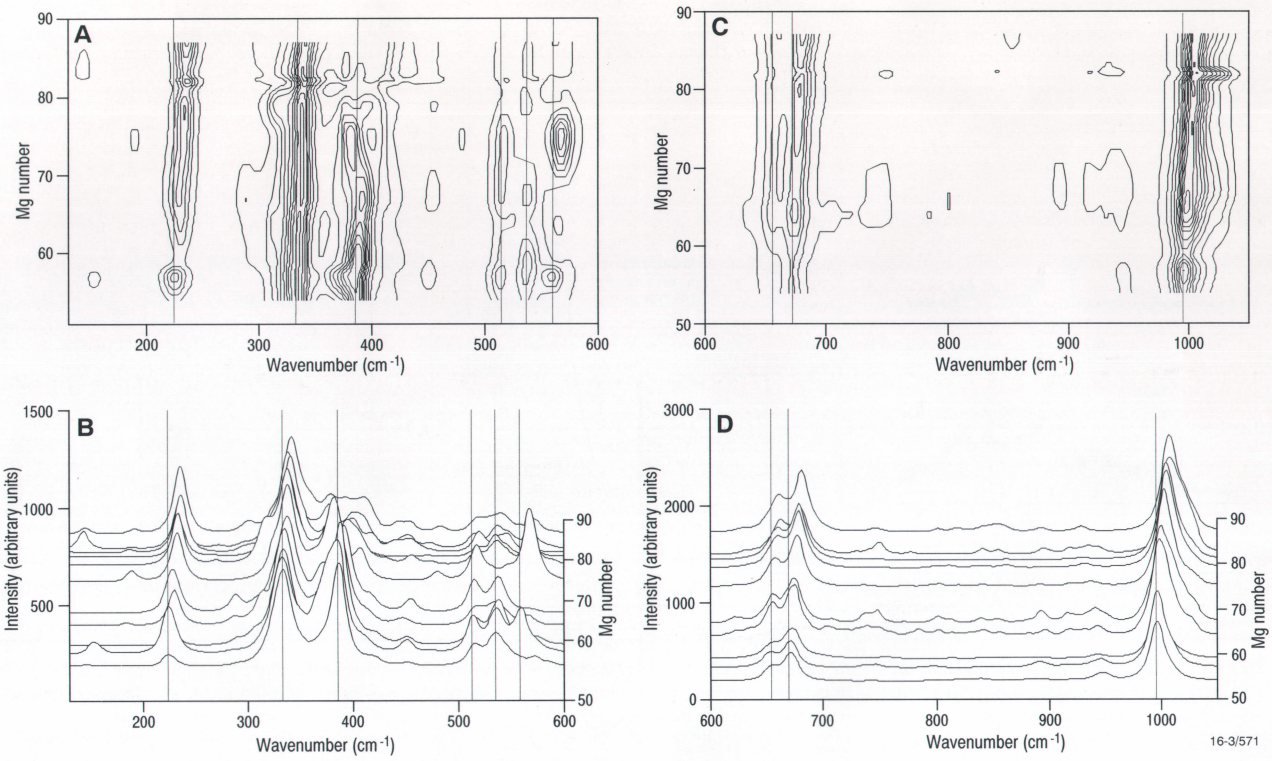

Fig. 5. Raman spectroscopic data for orthopyroxene and the inverted pigeonite host component from mg_{54} to mg_{87}. (A) Contour diagram showing the relationship between *mg* number and the wave number of the major Raman bands over the region 100–610 cm^{-1}. (B) Raman-microprobe spectral profile for each sample from 100–610 cm^{-1}. All spectra have been normalised using the band near 341 cm^{-1}.(C) Contour diagram showing the relationship between *mg* number and the wave number of the major Raman bands over the region 600–1040 cm^{-1}. (D) Raman-microprobe spectral profile for each sample from 600–1040 cm^{-1}. All spectra have been normalised using the band near 1008 cm^{-1}. Vertical straight lines have been added for reference.

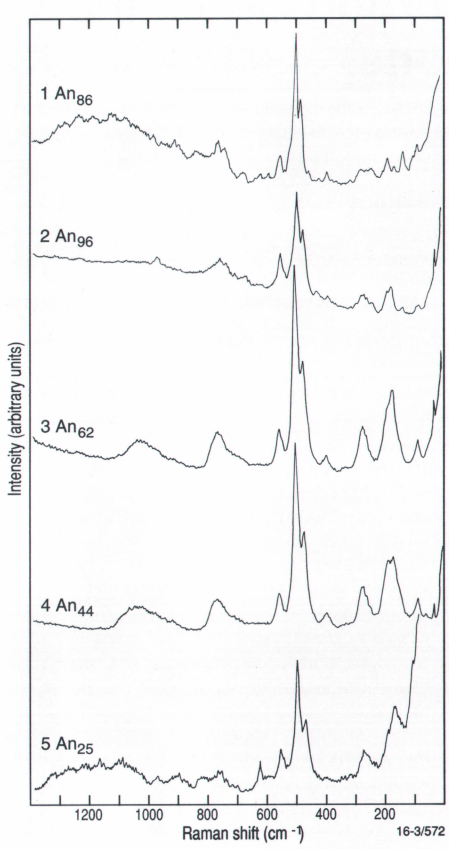

Fig. 6. Laser-Raman-microprobe spectra of the plagioclase minerals: (1) bytownite [An_{86}], (2) anorthite [An_{96}], (3) labradorite [An_{62}], (4) andesine [An_{44}], and (5) oligoclase [An_{25}].

tration depth of the Raman microprobe, however, makes it a suitable alternative for the identification of sulphides.

Raman spectroscopy can distinguish between various polymorphs. The two different spectra for pyrite (Fig. 7) are surprising, but this has been explained by the possible existence of both isotropic and anisotropic pyrite (Mernagh & Trudu 1993: *Chemical Geology*, 103, 113-127). The

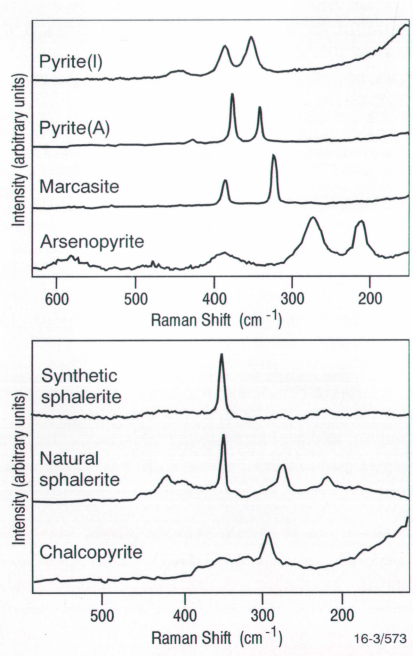

Fig. 7. Laser-Raman-microprobe spectra of sulphide minerals, including anisotropic (A) and isotropic (I) pyrite.

presence of impurities in these minerals can enhance the second-order Raman spectrum, as shown for natural sphalerite (Fig. 7), but it does not affect the frequencies of the first-order spectrum, and hence still permits ready identification of each mineral. Some caution is required when using the laser microprobe for the study of sulphides since the high-intensity focused laser radiation may result in thermal decomposition or oxidation of some of the more reactive minerals. Unless the spectra are collected at moderately

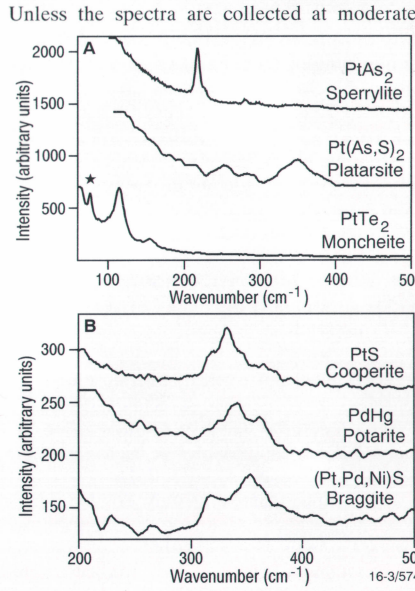

Fig. 8. Laser-Raman-microprobe spectra of platinum-group minerals with (A) cubic or trigonal symmetry, and (B) tetragonal symmetry. The star denotes a laser plasma emission.

low laser powers, a drop of deionised water should be placed on top of the specimen to help dissipate the heat and prevent thermal degradation.

PGMs

As mentioned above, the Munni Munni Complex also hosts PGMs, which — except for the Pt–Pd sulpharsenides — are all less than 10 μm in average grainsize. Owing to the problems (mentioned above) associated with the analysis of such minute grains by more conventional techniques, the laser Raman microprobe was used to identify PGMs in the mineralised layer of the Munni Munni Complex (Mernagh & Hoatson in press: *Canadian Mineralogist*). Like the sulphides, all the observed Raman bands for PGMs lie in the region below 500 cm^{-1}, and each mineral produces a distinct Raman spectral fingerprint (Fig. 8).

Conclusions

The above examples show that the laser Raman microprobe can be used to identify many of the common silicate or sulphide minerals, as well as the smaller (<10 μm) PGM grains which may occur in layered intrusions such as the Munni Munni Complex. As this is also a structure-sensitive technique it can discriminate between polymorphs and identify structurally anomalous crystals. This vibrational spectroscopic technique does not provide a chemical composition, so an electron or proton microprobe is still required to obtain these data. Even so, the laser Raman microprobe provides a convenient high-resolution (spot sizes down to 1 μm) rapid technique for the positive identification of minerals within a specimen or thin section.

For further information, contact Drs Terry Mernagh or Dean Hoatson (Division of Regional Geology & Minerals) at AGSO.

Preservation of old accumulations — key to Canning hydrocarbon exploration

Geohistory analysis of the onshore Canning Basin succession indicates that Palaeozoic organic-rich rock intervals attained peak maturity and expelled the bulk of their generated hydrocarbons during major subsidence-sag phases in either the

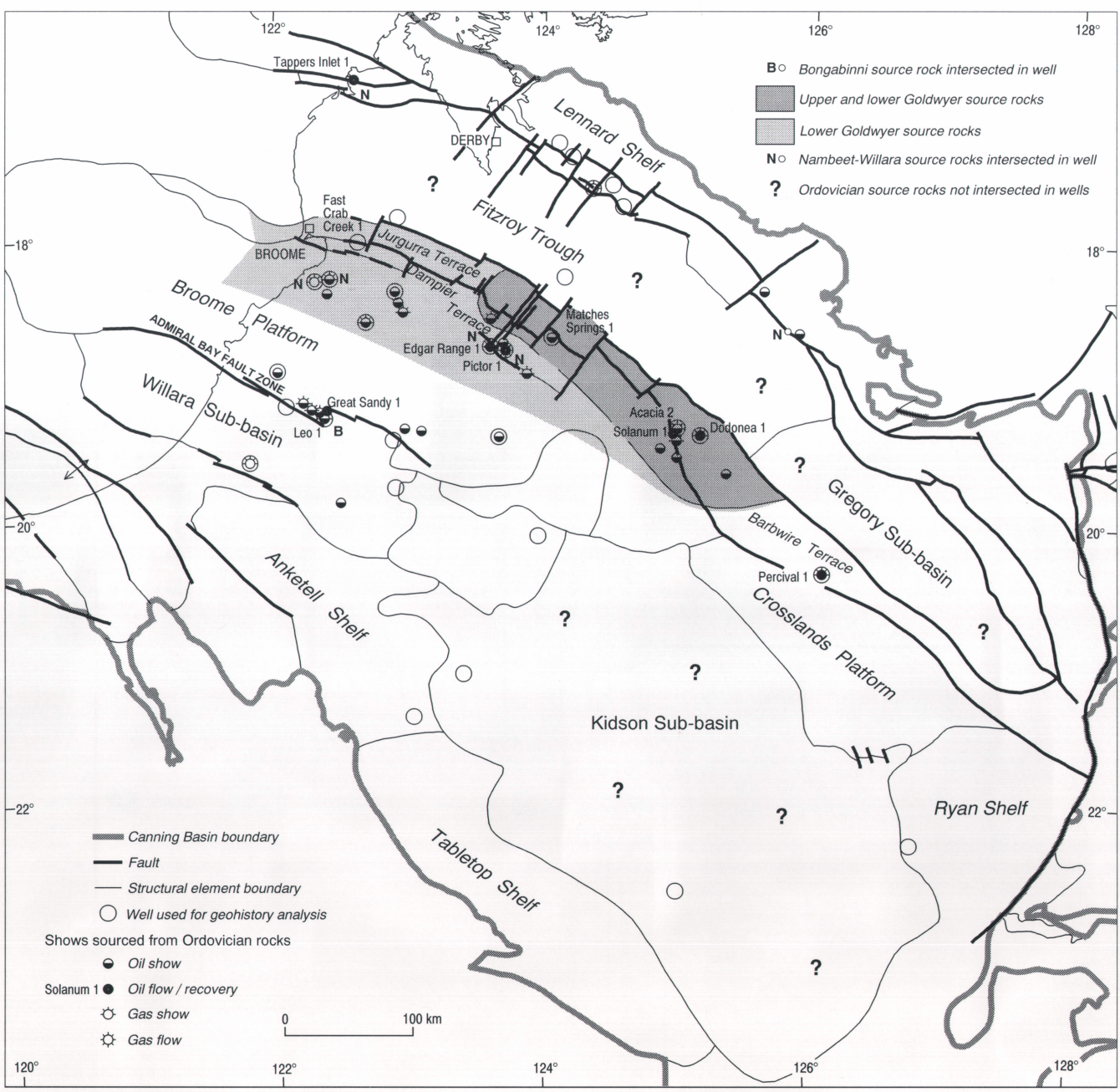

Fig. 9. Distribution of Ordovician source-rock intervals in the Canning Basin, and locations of wells used for geohistory analysis. Structural subdivisions are based on the 1:2 000 000 'Structural elements map of the Canning Basin' by Shaw et al. (1994: *AGSO Record* 1994/48).

Ordovician–Silurian, Middle Devonian–Early Carboniferous, or Early Permian–Triassic. Little or no additional generation and expulsion has occurred since the Triassic. Successful exploration for accumulations of hydrocarbons generated from these sources thus depends on suitable traps having been in place at these times, and, perhaps more significantly, adequate seal integrity and preservation of accumulations since that time.

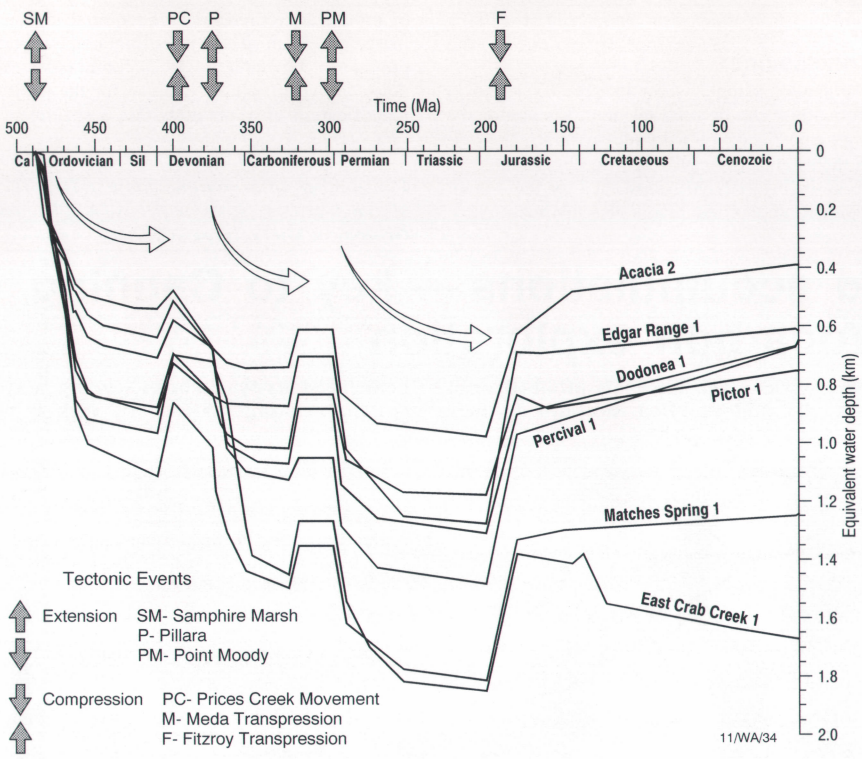

Fig. 10. Stripped-basement subsidence curves for wells modelled on the Jurgurra–Dampier–Barbwire Terraces, showing major tectonic events and subsidence-sag phases (curved arrows) that controlled thermal maturation of source intervals.

Thirty representative wells from most of the major structural elements of the basin (Fig. 9) have been modelled using the WinBury 1.4 geohistory analysis program. Recent biostratigraphic, geological, and structural studies undertaken by AGSO underpin this geohistory analysis; these studies have developed a thorough regional understanding of the stratigraphic and tectonic development of the basin, and of the evolution of the basin's petroleum systems.

Six major tectonic events have had a profound effect on the thermal history of the Palaeozoic source intervals (Fig. 10): three extensional events (Samphire Marsh, Pillara, and Point Moody Extensions) resulted in major subsidence-sag phases, each terminated by a major phase of uplift and erosion (Prices Creek Movement, Meda Transpression, and Fitzroy Transpression, respectively). Palaeoheat-flow models developed for the Palaeozoic are consistent with the geologic history of the basin and with observed maturity data, especially conodont-colour-alteration indices determined for the Ordovician succession by Nicoll (1993: *AGSO Record* 1993/17).

Of six Ordovician–Carboniferous organic-rich rock intervals identified in the basin, five appear to have generated and expelled hydrocarbons.

Ordovician source intervals

New kerogen kinetic data have highlighted the occurrence of significant spatial and temporal variations in original source richness and kerogen types within four Ordovician source intervals, designated the lower A1, lower and upper A2, and lower B1 supersequences by Kennard et al. (1994:

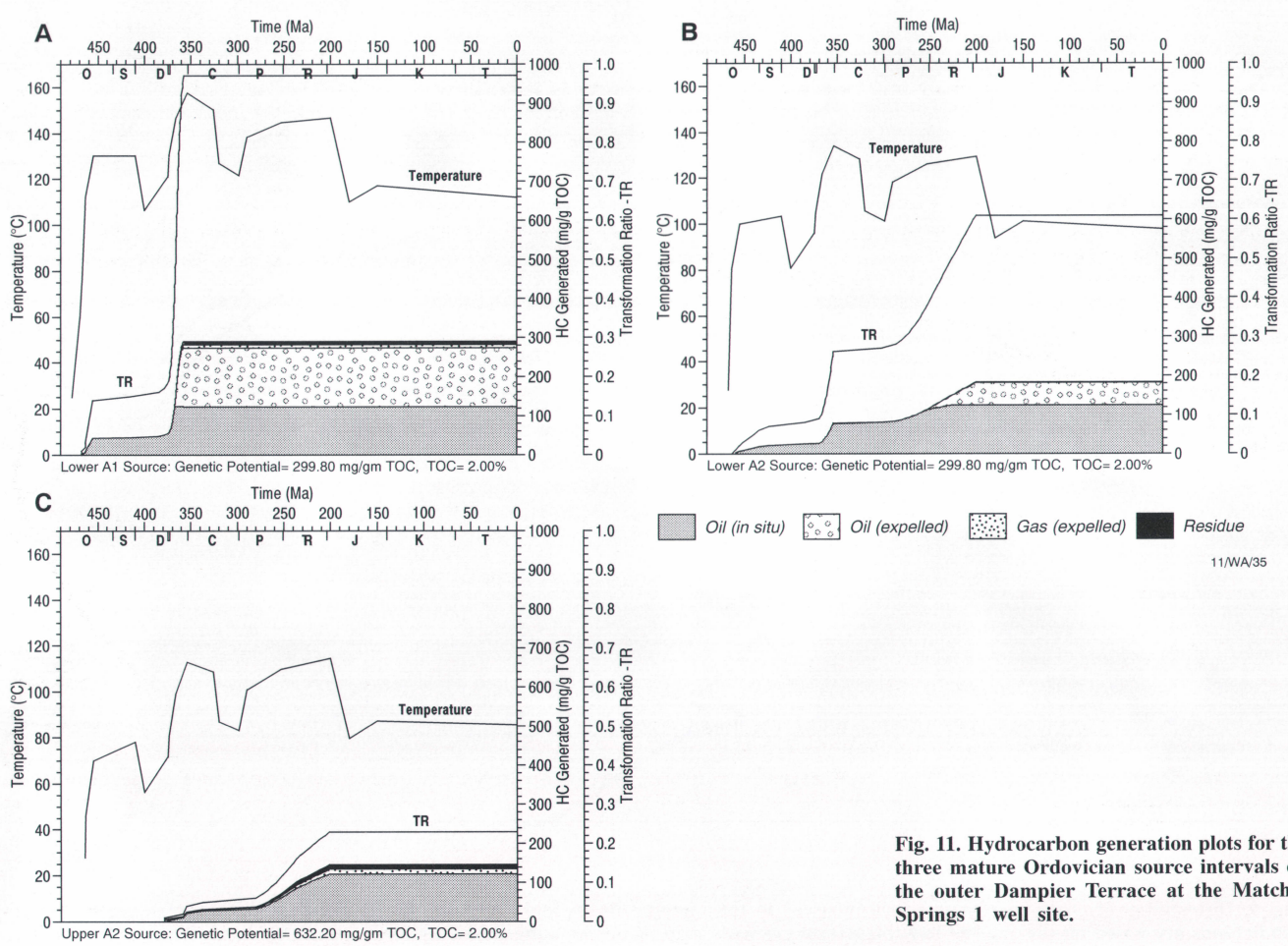

Fig. 11. Hydrocarbon generation plots for the three mature Ordovician source intervals on the outer Dampier Terrace at the Matches Springs 1 well site.

in Proceedings of the West Australian Basins Symposium, *Petroleum Exploration Society of Australia, Perth*, 657–676).

Hydrocarbon generation and expulsion from the three mature Ordovician source intervals — the lower A1 (Nambeet–Willara Formation), lower A2 (lower Goldwyer Formation) and upper A2 (upper Goldwyer Formation) — is probably limited to the Dampier–Jurgurra Terrace, outer Barbwire Terrace, and northern Fitzroy Trough. Peak generation of the oldest, lower A1 source on these terraces (Fig. 11a) probably occurred during the Devonian–Early Carboniferous depositional cycle (before the Meda Transpression), whereas peak generation in the Fitzroy Trough occurred in the Middle Ordovician (before the Prices Creek Movement). This interval probably did not generate large amounts of oil on the Broome Platform during either the Ordovician–Silurian or subsequent depositional cycles.

Peak generation of the lower A2 source interval probably occurred during the Devonian–Early Carboniferous (before the Meda Transpression) on the Jurgurra Terrace, and during the Triassic (before the Fitzroy Transpression) on the shallower Dampier Terrace (Fig. 11b). Minor generation with little or no expulsion occurred in deeper portions of the Barbwire Terrace during the Devonian–Early Carboniferous, and, provided suitable source facies are present, significant generation may have occurred in the southern Fitzroy Trough at this time. Again, this interval probably did not generate large amounts of oil on the Broome Platform during either the Ordovician–Silurian or subsequent depositional cycles.

Peak generation of the upper A2 source interval, the richest petroleum source in the basin, probably occurred during the Devonian–Early Carboniferous (before the Meda Transpression) in the Fitzroy Trough, and during the Triassic on the eastern Jurgurra–Dampier and outer Barbwire Terraces (Fig. 11c). Foster et al. (1986: *APEA Journal*, 26(1), 142–155) estimated that under optimal maturation conditions this interval has the potential to generate 61 x 10^9 barrels of liquid hydrocarbons on the Barbwire Terrace alone.

The newly identified Late Ordovician lower B1 (Bongabinni Formation) source interval is immature in the Admiral Bay Fault Zone, the only area where it has been identified. It probably requires burial of about 2000 m to generate hydrocarbons in this area. Local maturation of this source by migrating hydrothermal fluids may explain the occurrence of numerous oil shows in this area, including the oil recovered in Leo 1 and Great Sandy 1 wells.

Upper Palaeozoic source intervals

Oil (and minor gas) generation and expulsion from the Givetian–Frasnian lower D source interval (Gogo Formation and equivalent restricted carbonates facies) occurred throughout the Fitzroy Trough in the Late Devonian–Early Carboniferous, before the Meda Transpression. Significant generation also occurred on the Laurel Downs and Jurgurra Terraces at this time, and again during the Permian–Triassic before the Fitzroy Transpression. Peak generation on the Lennard Shelf and Dampier–Barbwire Terraces also occurred during the Permian–Triassic.

Oil and gas generation from the Tournaisian lower F source interval (lower Laurel Formation) occurred in the southern and central Fitzroy Trough during the Early Carboniferous, before the Meda Transpression. Generation probably also commenced on the Jurgurra Terrace at that time. Peak generation in the northern Fitzroy Trough and Jurgurra Terrace possibly occurred in the Triassic, immediately before the Fitzroy Transpression. Thus the large anticlinal structures formed during the Fitzroy Transpression, which have previously been regarded as prospective traps, are unlikely to be charged by this source.

Key hydrocarbon-preservation factors identified by the study

Geohistory analyses have provided new insights into the distribution, structural partitioning, original kerogen type, and time of hydrocarbon generation and expulsion of these source intervals. The work has highlighted the need for more reliable maturity parameters throughout the basin succession, especially within the Ordovician–Silurian section. The study suggests that the key critical factor yet to be systematically evaluated for successful exploration of the basin is seal integrity.

Details of this geohistory analysis were recently published by Kennard et al. (1994: *AGSO Record* 1994/67, 243 pp.).

For further details, contact John Kennard or Jim Jackson (Division of Marine, Petroleum & Sedimentary Resources) at AGSO.

High-precision geochronology of Palaeoproterozoic layered mafic–ultramafic intrusions in the East Kimberley

The Palaeoproterozoic layered mafic–ultramafic intrusions in the East Kimberley have attracted considerable exploration interest for occurrences of platinum-group-elements (PGEs), Cr, Ni, Cu, Co, and Au. However, there have been few attempts to identify different phases of mafic–ultramafic magmatism and associated mineralisation on a regional scale. High-precision U–Pb zircon ages of fractionated anorthositic and gabbroic cumulates reported here indicate that the prospective Panton, Springvale, and Toby layered intrusions were emplaced over a short time period at 1855–1857 Ma, and that the large McIntosh intrusion was emplaced at 1830 ± 3 Ma. The ~1855-Ma layered intrusions are broadly coeval with the felsic Whitewater Volcanics and associated granites of the Bow batholith (~1850–1860 Ma).

A recent geochronological study of the Palaeoproterozoic of the East Kimberley has obtained ages for zircon from cumulate rocks, and from migmatite formed during emplacement of another layered intrusion. This study is part of the Kimberley–Arunta National Geoscience Mapping Accord project being carried out by AGSO and the Geological Survey of Western Australia.

The layered mafic–ultramafic intrusions in the East Kimberley were collectively grouped by Dow & Gemuts (1969: *BMR Bulletin* 106) into the Alice Downs Ultrabasics and the McIntosh Gabbro. However, contact relations with country rocks, degrees of fractionation, styles and intensities of deformation, and types of associated mineralisation indicate that these intrusions are of several different types and ages. Field relations and U–Pb geochronological data show that the intrusions can be assigned to seven main groups, at least three of which appear to be coeval (Fig. 12).

Fractionated anorthosites and high-Zr-bearing gabbros (containing up to 140 ppm Zr) were sampled from five potentially economic layered intrusions for U–Pb zircon dating (using the SHRIMP II ion-microprobe located in the Research School of Earth Sciences, Australian National University). The Panton and Sally Malay mafic–ultramafic intrusions contain the largest resources of PGE–Cr–Ni–Cu–Au and Ni–Cu–Co, respectively, in the East Kimberley. The Springvale and Toby mafic intrusions host minor amounts of chromite, and the large McIntosh mafic intrusion has potential for Ti–V and Au resources (Hoatson & Tyler 1993: *AGSO Research Newsletter* 18, 8–9; locations of intrusions dated are shown in fig. 10 of Hoatson 1993: *AGSO Research Newsletter*, 19, 9–10).

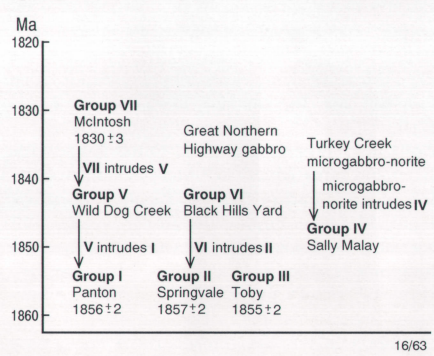

Fig. 12. Preliminary temporal relationships of mafic–ultramafic intrusions from the Halls Creek Orogen.

Those intrusions forming large layered bodies are assigned to groups I to VII. The type example of each group is annotated, and its U–Pb zircon age, where determined, is also indicated (see figure 10 of Hoatson 1993: *op. cit.*, for the locations of the intrusions). The Great Northern Highway gabbro and Turkey Creek microgabbro–norite, which have not been dated, typically form poorly layered irregular bodies.

Panton intrusion (group I)

The Panton mafic–ultramafic intrusion is a synclinally folded body that consists of a lower ultramafic series, 650 m thick, of olivine and chromite cumulates, and an overlying gabbroic series, 900 m thick, of gabbro, norite, anorthosite, and ferrogabbro. On its southern margin the Panton body intrudes gneissic granite dated at 1863 ± 3 Ma (Rose Bore Granite in the Panton River) and older metasediments. Zircons from a mottled anorthosite in the upper part of the gabbroic series in the Panton intrusion are somewhat altered, squat euhedral grains that have high U (2000–5000 ppm) and very high Th/U. They form a single concordant data set indicating a U–Pb age of 1856 ± 2 Ma, interpreted as the time of igneous crystallisation for the Panton intrusion.

Springvale (group II)

The Springvale intrusion is a moderately dipping mafic sheet ~2 km thick comprising olivine gabbro, gabbronorite, troctolite, and anorthosite. A population of clear subhedral to shapeless zircons was extracted from a mottled anorthosite hosting disseminated chromite in the northwestern part of the intrusion. These zircons have only moderate U contents (230–1500 ppm) but higher Th/U than the Panton zircon suite. The zircon U–Pb data set is concordant, and indicates an igneous crystallisation age of 1857 ± 2 Ma for the Springvale intrusion.

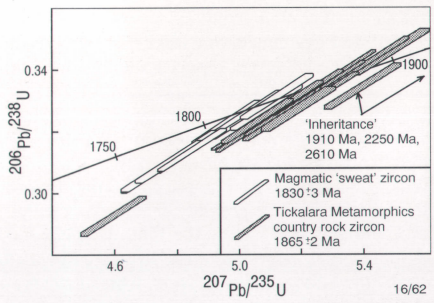

Fig. 13. Concordia plot of zircon U–Pb data from the contact zone of the McIntosh intrusion.

Thirteen data points define the age of 1830 ± 3 Ma from the felsic melt (leucosome) fraction of the contact migmatite, and this is regarded as the emplacement age of the mafic intrusion. The Tickalara Metamorphics country rock contains zircon age components at 1865 ± 2 Ma, 2250 Ma, and 2610 Ma. Error boxes are 1-sigma analytical uncertainties, and quoted age errors are 95% confidence limits.

Toby (group III)

The Toby mafic intrusion forms a gently dipping basinal body ~3 km thick that is areally the largest intrusion in the East Kimberley. Part of a high-level subophitic quartz–biotite gabbro unit with an anomalous Zr content (90–140 ppm) from the central part of the intrusion was dated. The sample analysed contains clear inclusion-free, light brown zircons which, unlike the Panton and Springvale suites, are generally not euhedral and have normal Th/U and U (100–500 ppm). However, the zircon crystallisation age determined for the Toby intrusion (1855 ± 2 Ma) is indistinguishable from the age of the other two intrusions.

Sally Malay (group IV)

The Sally Malay mafic-ultramafic intrusion is a small multichambered body consisting of cyclic units of peridotite, troctolite, olivine gabbro, and anorthosite. A sample of mottled anorthosite from the upper part of the lowest cycle that hosts basal segregations of Ni–Cu–Co sulphides contains both primary zircon and baddelyite (ZrO_2). U–Pb analyses will be undertaken on these two minerals to date this intrusion. Currently, the group IV Ni–Cu mineralised intrusions are tentatively considered to be younger than the group I–III bodies (Fig. 12).

McIntosh (group VII)

The McIntosh intrusion is a thick (7.8 km) mafic body consisting of cyclic units of olivine gabbro, olivine gabbronorite, troctolite, magnetite gabbro, and minor peridotite. Gabbro from the northwestern basal contact of the intrusion lacks zircon or baddelyite, so cannot be directly dated. However, garnet-bearing paramigmatite formed in the contact aureole of the intrusion evinces considerable partial melting, and zircon crystallised in resultant leucosome bands affords an indirect means of determining the emplacement age of the mafic intrusion.

The zircon U–Pb data fall into two clear groups (Fig. 13). The younger defines an age of 1830 ± 3 Ma, interpreted as the time of contact metamorphism/partial melting, and hence the age of emplacement of the McIntosh intrusion. Older zircon populations in the migmatite reflect provenance of the country rock (Tickalara Metamorphics paramigmatite); the dominant population at 1865 ± 2 Ma represents its maximum depositional age.

Conclusions

The new geochronological data for the layered mafic–ultramafic bodies of groups I–III show that they were emplaced over a brief period around 1855 Ma, 25 Ma before the group VII McIntosh intrusion was emplaced. The older layered intrusions are therefore contemporaries of some of the felsic rocks of the Bow batholith and Whitewater Volcanics. Together, this mafic and felsic magmatism (~1850–1860 Ma) represents a major pulse of heat into the Earth's crust during the development of the Halls Creek Orogen.

These new zircon ages and the chemical compositions of the mafic–ultramafic bodies have implications for the tectonic environment, and mechanism for magmatism and regional metamorphism in the East Kimberley. Estimated chemical compositions for the parent magmas of the mafic–ultramafic bodies are generally tholeiitic, similar to some modern intraplate continental flood basalts (and to the nearby 1800-Ma Hart Dolerite). Sun et al. 1991 (*Precambrian Research*, 50, 1–35) have suggested that they were produced at low pressure by large-scale partial melting of lithospheric mantle in an intraplate environment.

For further information, contact Drs Rod Page, Dean Hoatson, Shen-su Sun, or Mr Chris Foudoulis (Division of Regional Geology & Minerals) at AGSO.

The Lakefield Basin

A newly named Permian basin in far north Queensland

A re-evaluation of geological and geophysical data shows that the broad shallow Mesozoic Laura Basin on Cape York Peninsula overlies a deep elongate basin, called here the Lakefield Basin. The north-striking Lakefield Basin has a Permian to mid?-Triassic sedimentary fill up to 10 km thick, and is 70 km wide and at least 200 km long. Although these rocks have been recognised by previous workers (e.g., Pinchin, 1974: *Journal of the Geological Society of Australia*, 21, 437–445), the extent and significance of the basin have not been described previously.

Basin extent

The Lakefield Basin is indicated by the following:

- Permian rocks at the bases of the five oil/stratigraphic wells drilled through the western Laura Basin, and at the bases of coal-survey holes in the northeastern Laura Basin (Fig. 14);
- dipping seismic reflections and their extrapolation to zero thickness below the western Laura Basin (Figs. 15 and 16)
- a low gravity anomaly reflecting thick low-density sedimentary rocks in the area of the western Laura Basin (Fig. 14); and
- an area below the western Laura Basin that contains saucer-shaped magnetic anomalies (7–30 km diameter; Fig. 14) due to lenticular igneous bodies within the Lakefield Basin.

The western margin of the Lakefield Basin has been mapped from the inflexion of the gravity anomalies, the eastward extent of short-wavelength magnetic anomalies, and, most importantly, an abrupt eastward reduction in upper-crustal apparent susceptibility indicated by the reduced-to-the-pole magnetic anomalies.

The eastern margin of the Lakefield Basin is apparent from the distribution of Permian(–?Triassic) rocks, and older rocks (Hodgkinson Formation and granite) of the Hodgkinson Province, in coal-search drillholes and in outcrop; and from the interpreted position of the subcropping Palmerville Fault (Fig. 14).

South of the Laura Basin, the Palmerville Fault crops out as a major lineament that separates Proterozoic metamorphic rocks in the west from Palaeozoic Hodgkinson Province rocks in the east. Locally divergent branches of this fault also incorporate as a sliver one of two Permian formations (Lakefield Basin correlatives: Little River Coal Measures and Normanby Formation) that crop out near the southern margin of the Laura Basin (Fig. 14). Fault-parallel outcrops of the Chillagoe Formation adjacent to the Palmerville Fault and Little River Coal Measures outcrop coincide with narrow intense positive magnetic highs. Magnetic highs with similar wavelengths traceable northwards as far as the coast at about longitude 144°20'E in Princess Charlotte Bay (Fig. 14) reflect the Chillagoe Formation subcrops beneath the Laura Basin.

Again in the Hodgkinson Province, gravity lows correlate in areas of outcrop with mainly S-type Permo-Carboniferous granitoids. Farther north, in the Laura Basin area, similar gravity lows are abruptly truncated near the western edge of the narrow belt of inferred Chillagoe Formation subcrops beneath the Laura Basin (Fig. 14).

The foregoing observations suggest that the Palmerville Fault and rocks outcropping along the western margin of the Hodgkinson Province subcrop beneath the Laura Basin with a strike just east of north, and that the eastern margin

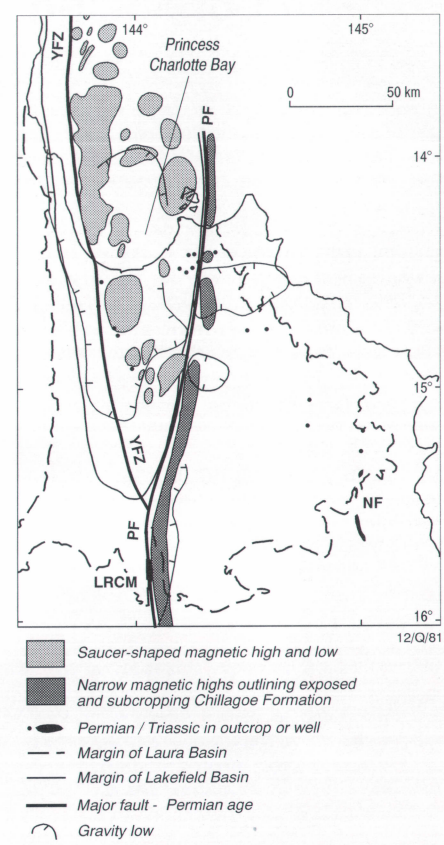

Fig. 14. Controls on the extent of the Lakefield Basin.

Major faults are the Palmerville Fault (PF), and the Yintjingga Fault Zone (YFZ). Other outcropping Permian sedimentary rocks are the Normanby Formation (NF) and Little River Coal Measures (LRCM).

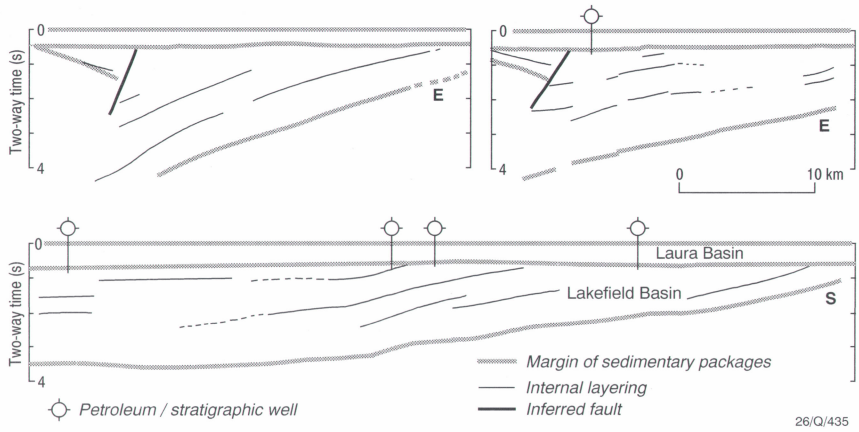

Fig. 15. Line drawings of seismic reflection profiles through the Laura and Lakefield Basins. The two upper sections strike east–west, and the lowest section strikes north–south.

of the Lakefield Basin coincides with the Palmerville Fault.

Depth and structure of the basin

Seven seismic reflection surveys for hydrocarbons have covered parts of the Laura Basin onshore and offshore, but the offshore surveys did not satisfactorily image reflections below the Laura Basin. The onshore surveys showed that a gently dipping layered sucession of rocks extends to over 4 s two-way travel time beneath the Laura Basin (Fig. 15). A major fault (part of the Yintjingga Fault Zone; Fig. 14) separates a thin, east-dipping section in the west, from a thick west-dipping section in the east. Reflectivity in both sections varies from areas with no or poor reflections to areas with well-spaced, strongly reflecting continuous horizons, but prominent reflectors are common near the bases of both sections.

Time–depth relations applied to map the depth of the base of the Lakefield Basin are based on the average VRMS (velocity root-mean-squared) velocities identified in the seismic profiles of the 1989 Kalpower survey: 4.5 km.s^{-1} at 1 s, and 5.25 km.s^{-1} at 2.8 s. The high reflection velocity for these rocks is supported by seismic refraction velocities for the rocks at the top of the sections: 5.4 km.s^{-1} east of the fault, and 4.2 km.s^{-1} west of the fault. Depths to the bases of the Laura and Lakefield Basins (Fig. 16) are based on the seismic reflection data, except in the eastern part of the Laura Basin, where they are based on drilling information and depth to magnetic basement.

Age and lithology

The uppermost part of the thick Lakefield sequence has been intersected in five oil exploration/stratigraphic wells. These holes bottomed in clastic rocks, volcanics, and granite which are thought to be Permian for the following reasons:

- Permian spores and pollen in Ebagoola 1 and Broken Rope 1;
- Glossopteris indica in Marina 1;
- lithological similarity with the Upper Permian Normanby Formation; and
- the apparent Carboniferous–Permian nature of the granitoid in Lakefield 1.

However, some outcropping sedimentary remnants within a 200-km radius range in age from Permian to Triassic, and in Ebagoola 1 the Laura Basin sequence contains reworked miospores of both Permian and Triassic ages, so the eroded-off former upper part of the Lakefield Basin may be as young as Triassic.

The clastic rocks in these wells are shale, siltstone, sandstone, and minor conglomerate. The sandstone and siltstone are indurated and have quartz-grain overgrowths; some of the shale is extremely carbonaceous and has 'large gas peaks', but is overmature for petroleum (Willis 1991: Broken Rope 1, ATP 368P, well completion report, *Crusader Limited, unpublished*).

Initiation of the Lakefield and Laura Basins

The available data are not adequate to establish a detailed model for the formation of the Lakefield Basin. The main section does not thicken much in any direction, so there is no strong evidence for a half-graben origin. Also, this sedimentary pile, ~10 km thick, is unlikely to have accumulated over a large part of the region surrounding the Lakefield Basin. The basin-forming subsidence is thought to have been due to some form of crustal extension. If so, the consequent cooling of the lithosphere and the accompanying thermal subsidence would have resulted in the formation of an overlying thermal-sag basin. A thermal subsidence origin for the Laura Basin is indicated by this reasoning, by the shapes of the basins, and by the short time interval between the two periods of sedimentation (Middle? Triassic to Middle? Jurassic).

Conclusions

The information outlined has two important implications for the regional tectonics of Cape York Peninsula:

- the Late Carboniferous–Permian interval is an important period of both igneous activity and thick sedimentation; and
- the Palmerville Fault, forming the western margin of the Hodgkinson Province, swings about 70 km east of its previously interpreted position.

For further information, contact Dr Peter Wellman (Division of Regional Geology & Minerals) at AGSO.

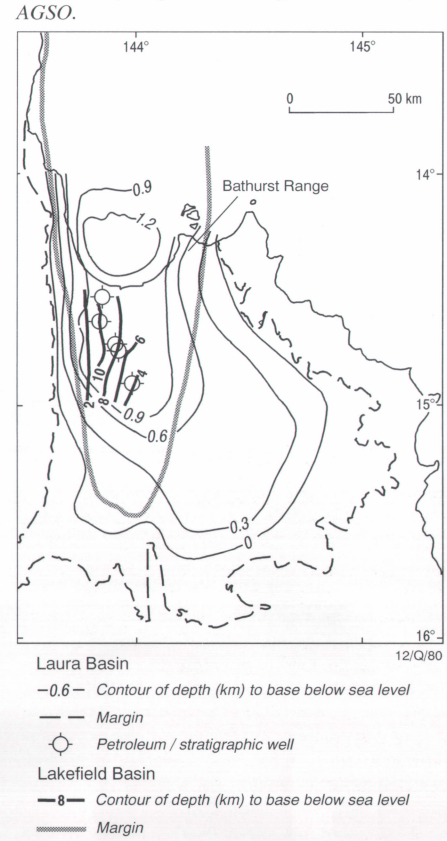

Fig. 16. Extents and depths of the Lakefield and Laura Basins.

New mineral discoveries in the East Kimberley

As part of its contribution to the Kimberley-Arunta National Geoscience Mapping Accord (NGMA) project, AGSO has identified some previously undocumented mineral occurrences of potential economic significance in Palaeoproterozoic rocks in the McIntosh and Turkey Creek 1:100 000 Sheet areas of the East Kimberley. These include stratiform sulphide layers and ilmenite lenses within layered mafic–ultramafic intrusions, and folded banded-iron formation in a sequence of mafic–felsic metavolcanics and metasediments. These occurrences, which have prominent surface expressions and geophysical–geochemical signatures, show that the Halls Creek Orogen of the East Kimberley still has potential for the discovery of outcropping mineral deposits.

Stratiform sulphide mineralisation in the Norton intrusion

Iron-rich gossans along the basal contacts of Palaeoproterozoic layered mafic–ultramafic intrusions in the East Kimberley have been a focus for Ni–Cu–Co-sulphide exploration. For example, at the Sally Malay, Dave Hill, Keller Creek, and McKenzies Spring prospects (locations shown in fig. 10 of Hoatson 1993: *AGSO Research Newsletter* 19, p. 9), subeconomic massive, disseminated, and remobilised sulphides occur in structural traps or embayments along the basal contacts beneath the thickest sequence of mafic–ultramafic cumulates. The gossans, indicating sulphide mineralisation at depth, are generally 1 to 5 m wide and have strike extents up to 200 m.

Similar products of mineralisation are indicated at the newly mapped metamorphosed Norton mafic intrusion, a north-northeasterly-trending lenticular body in the Violet Valley Aboriginal Reserve near the western margin of the Turkey Creek 1:100 000 Sheet area (Fig. 17). The Norton body covers an area of ~1.5 by 9.5 km, has a stratigraphic thickness of 1 km, and intrudes garnet ± cordierite paramigmatites of the Tickalara Metamorphics. Dominant rock types are hornblende metagabbro and hornblende–magnetite metagabbronorite (mafic granulites), and the upper part of the body is intruded by fine-grained

norite and microgabbro. High S concentrations of 1160–2700 ppm for the mafic granulites indicate that the Norton intrusion crystallised from S-saturated magmas.

The basal 80 m of the mafic sequence exposed in the northwest part of the Norton intrusion includes ferruginous gossans that persist intermittently along strike for at least 4 km (Fig. 17). In places, thin gossanous veins also cut the footwall paramigmatite, indicating some later remobilisation of the sulphides. X-ray diffraction studies show that the gossans contain goethite, hematite, traces of magnetite and/or maghemite, and — as the major silicate minerals — quartz and montmorillonite; no nickeliferous carbonate phases were detected. Maximum Ni and Cu concentrations for two analysed gossan samples are not markedly anomalous (80 and 140 ppm, respectively), which could indicate that either the gossans were derived from the oxidation of disseminated Ni–Cu poor, Fe-rich sulphide assemblages (e.g., pyrite and/or pyrrhotite), or that any base metals originally present have been leached by acidic groundwater. Further sampling and drilling is required to assess the economic significance of the gossans.

The lateral continuity of the gossans, their favourable stratigraphic position, and the proximity of similar Ni–Cu prospects indicates that the Norton intrusion has potential for basal segregations of Ni–Cu–Co-sulphides. The most prospective parts are considered to be embayments in the footwall contact (where sulphides might have accumulated by gravitational and/or thermal erosion/contamination processes) in the central part of the intrusion where the overlying cumulate sequence is thickest. The absence of layered ultramafic cumulates in the Norton intrusion does not downgrade the economic potential of the body; likewise, thick olivine-rich sequences are absent from nearby Corkwood and Keller Creek Ni–Cu prospects, and the host rocks of the Sudbury deposit in Ontario — the largest Ni-sulphide resource in the world — are mainly mafic rather than ultramafic.

Stratiform Ti–Fe oxide mineralisation in the Frog Hollow intrusion

The Frog Hollow mafic intrusion covers an area of ~0.8 by 11 km (Fig. 17) in the Violet Valley Aboriginal Reserve, and has a geological setting similar to the nearby Norton intrusion. However, it ranges in composition from melagabbro to anorthosite to ferrogabbro, and contains local concentrations of Ti–Fe oxides, so it is more fractionated than the Norton body.

Ferrogabbroic rocks in the upper southwestern part of the Frog Hollow intrusion contain the thickest lenses of Ti–Fe oxides known in the Kimberleys. The largest lens, ~20 m wide by 30 m long, contains deformed coarse aggregates of ilmenite (~55% vol.), secondary tremolite–actinolite (40%) after clinopyroxene, and minor titaniferous magnetite (5%). The ilmenite–clinopyroxene cumulate in this lens has high TiO_2 (39.4%), and total Fe as Fe_2O_3 (52.5%), V (0.23%), and Cr (0.08%). Another oxide lens lower down in the gabbroic stratigraphy contains less TiO_2 (22.1%), but more total Fe as Fe_2O_3 (60.6%), V (0.99%), and Cr (0.93%). These concentrations compare favourably with the main Australian titaniferous magnetite deposits associated with layered intrusions — which typically contain 3 to 30% TiO_2 and 0.1 to 0.7% V (1986 *Australian Mineral Industry Quarterly*, 39 (1), p. 7).

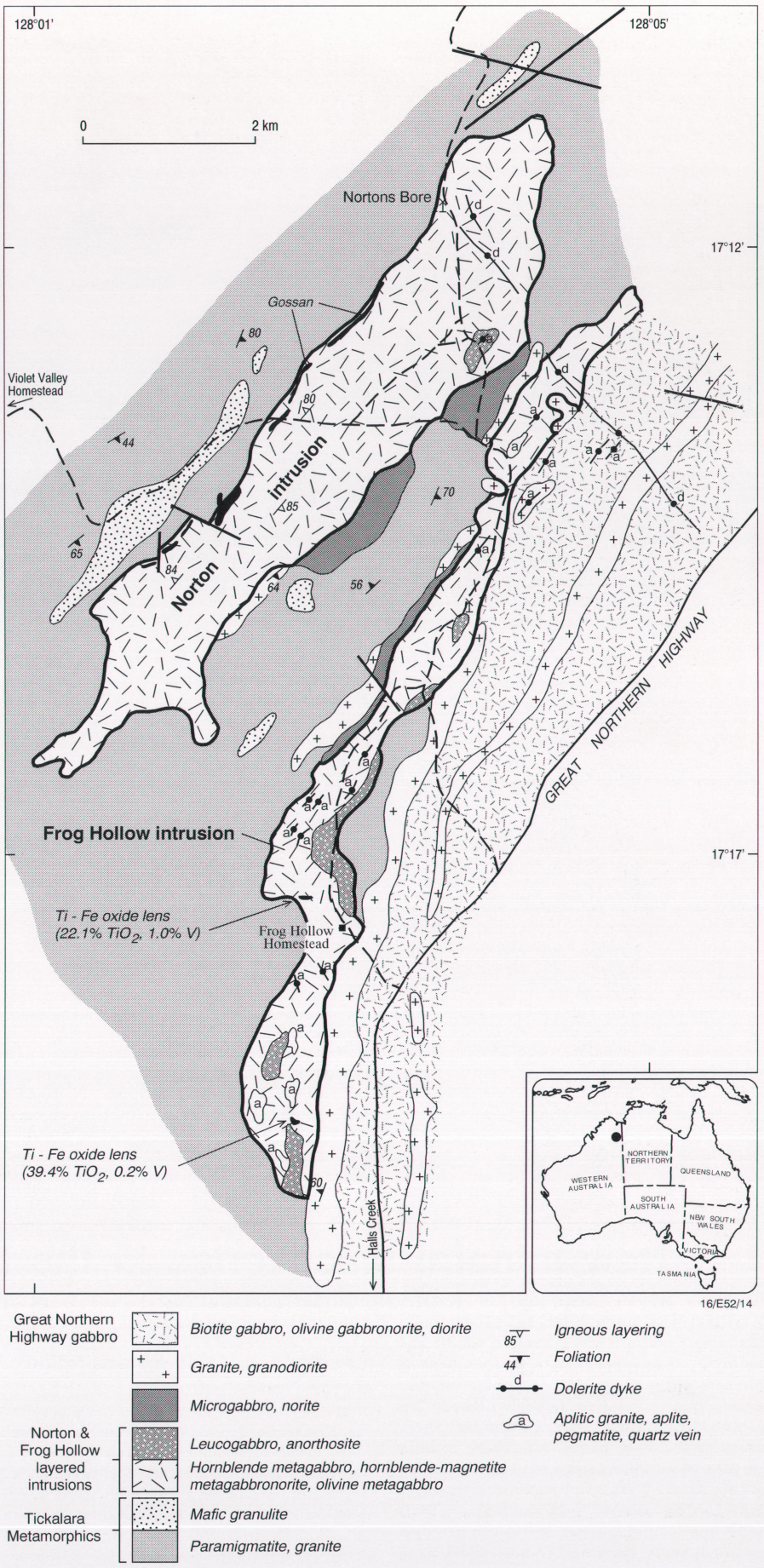

Fig. 17. Preliminary geology of the Norton and Frog Hollow mafic intrusions.

Upper Panton River banded-iron formation (BIF) occurrence

An intense aeromagnetic anomaly and a distinctive Landsat Thematic Mapper feature correspond to a prominent BIF exposed in the McIntosh 1:100 000 Sheet area (Fig. 18). The BIF is an elongate body, ~650 by 1200 m, within a sequence of metabasalt (including pillow lavas), iron-rich and chloritic schistose metasediments, dolomitic carbonates, and minor felsic volcanics. This sequence may belong to the Koongie Park Formation, isotopically dated at 1843 ± 2 Ma farther south near Halls Creek and the host to several volcanogenic base-metal deposits (Page et al. 1994: *AGSO Research Newsletter* 20, 5–7). Further geochronological data are required to determine if these rocks belong to the Koongie Park Formation or an older unit.

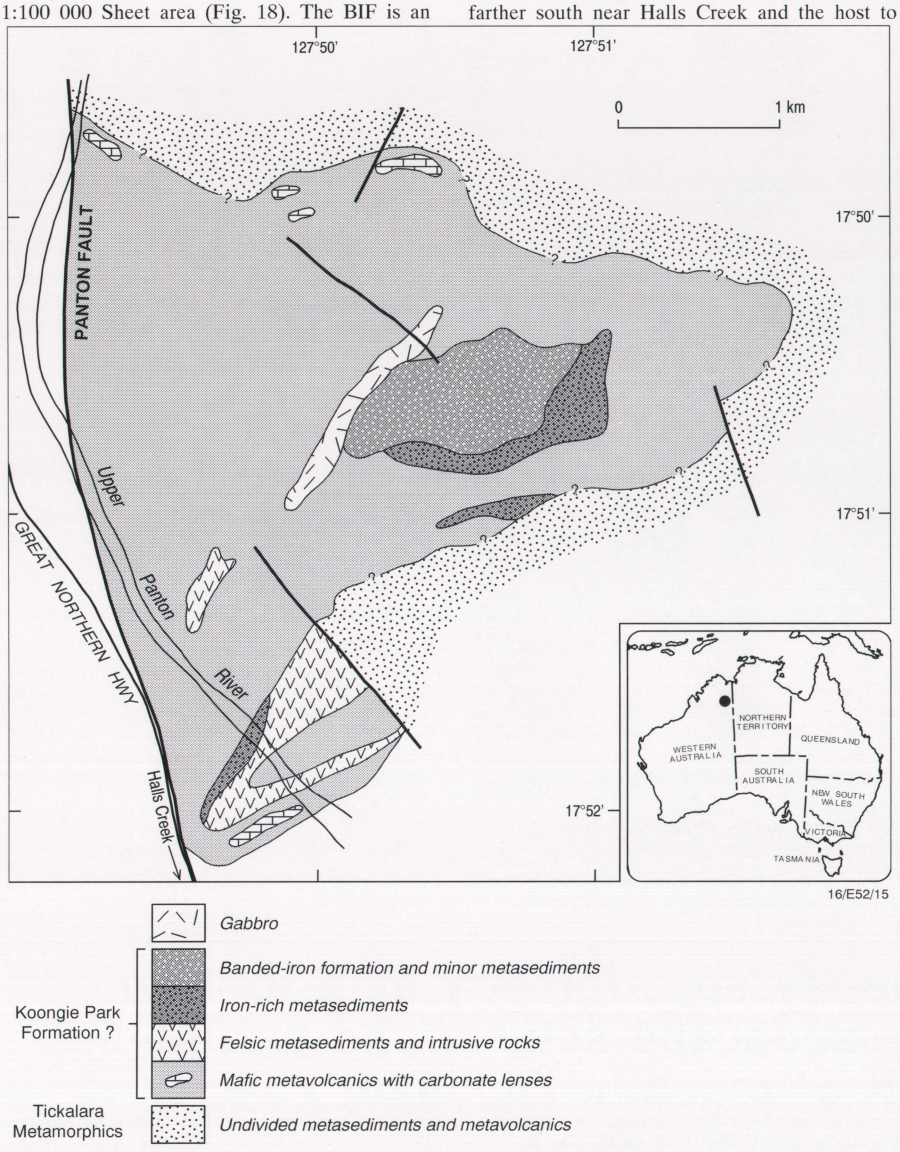

Fig. 18. Preliminary geology of the Upper Panton River banded-iron formation occurrence.

The BIF is finely laminated, and displays tight isoclinal folding on a centimetre to metre scale. X-ray diffraction studies show that hematite is the major iron phase, followed by magnetite and/or maghemite. Quartz, Fe-chlorite, and white mica are the dominant silicate phases, and siderite, barite, tourmaline, and ?grunerite are trace minerals. Maximum oxide concentrations in two composite BIF samples are 59.2% total Fe as Fe_2O_3 (41.4% Fe), 40.2% SiO_2, 2.33% Al_2O_3, and 1.33% P_2O_5 (0.58% P). If the two samples are representative of the total deposit, the low Fe and high P contents indicate that the Upper Panton River BIF has no potential for Fe, because the large iron ore deposits mined in the Hamersley Basin of Western Australia typically contain ~91.5% total Fe as Fe_2O_3 (64% Fe), 3.5% SiO_2, 2% Al_2O_3, 3% LOI, and less than 0.1% P (Pratt 1993: 'Australia's iron ore resources', *Bureau of Resource Sciences, Resource Report*). However, there may be potential for precious-metal enrichment (Au and/or platinum-group elements, PGEs) in the BIF, or volcanogenic base-metal deposits in the surrounding metavolcanics and metasediments.

Economic potential of the East Kimberley

The recent NGMA mapping has extended the known distribution of prospective rock types and metallogenic corridors for Ni, Cu, Co, PGEs, Cr, and Au occurrences in layered mafic–ultramafic intrusions (Hoatson 1993: *AGSO Research Newsletter* 19, 9–10; Hoatson et al. 1995: *AGSO Research Newsletter*, this number, front page). The Norton gossan and Frog Hollow Ti–V occurrences are located near the northeastern end of the Ni–Cu–Co metallogenic corridor of mineralised layered intrusions. The Upper Panton River BIF, if hosted by the Koongie Park Formation, extends the known distribution of this prospective formation north into the McIntosh Sheet area. The mapping has shown that different styles of potentially economic mineralisation with prominent surface expressions and geophysical–geochemical signatures are still to be found in the East Kimberley.

For further information, contact Dr Dean Hoatson (Division of Regional Geology & Minerals) at AGSO.

Late Palaeozoic magmatism in north Queensland: recent new perspective expanded by transfer-structure hypothesis

Wellman et al. (1994: *AGSO Research Newsletter*, 20, 8–9, figs. 9 and 10) described a newly recognised late Palaeozoic igneous zone in north Queensland — the Townsville–Mornington Island Igneous Belt (TMIIB) — traceable from off the east coast into the Gulf of Carpentaria. Although the TMIIB is rather diffuse, it is detectable for roughly 1000 km, and has an average width of about 100 km. Having an overall west-northwesterly trend, it crosses several roughly north-trending Proterozoic and pre-late Palaeozoic structural–stratigraphic provinces and subprovinces, or geophysical domains. The main western sector of the TMIIB (more than half of its total recognised length) is linear. The eastern sector (from roughly the margin of the Carpentaria Basin opposite Innisfail, to the Townsville area) is curvilinear, and increasingly assumes a conventional (for coastal north Queensland) north-northwesterly late Palaeozoic trend closer to Townsville. Where exposed (or intersected in drillholes, in the west) the TMIIB contains Carboniferous and Permian I- and A-type granitoids, accompanied by voluminous cogenetic ignimbrites. Volcanic and composite volcano-tectonic cauldrons are common (e.g., Branch 1966: *BMR Bulletin* 76; Oversby et al. 1980: *in* 'The geology and geophysics of northeastern Australia', *Geological Society of Australia, Queensland Division, Brisbane*, 247–268; Mackenzie 1993: *AGSO Record* 1993/82; Mackenzie et al. 1993: 'Geology of the Featherbed cauldron complex, Queensland', *AGSO 1:100 000-scale special map*).

The new perspective on Permian and Carboniferous magmatism (and associated mineralisation) in north Queensland afforded by initial recognition of the TMIIB is taken a step farther here by suggesting that the belt probably represents a fundamental extensional transfer structure, possibly activated in response to 'membrane' tectonics. Regional relationships among and between late Palaeozoic igneous rocks (below) support the contention that the belt is between, and transverse to, two regional-scale structural tracts, south and north of it, which reacted differently to Carboniferous–Permian extension. These suggestions expand, areally and conceptually, on ones originally presented by Oversby (1987: *BMR Record* 1987/51, pp. 233; 1988: *Geological Society of Australia, Abstracts*, 21, 307–308).

The TMIIB is near-orthogonal to exposed north–south late Palaeozoic stratigraphic and

structural trends, and partly coincident meridional gravity troughs (most conspicuously in and adjacent to the Newcastle Range, immediately south of the belt). These have been inferred to indicate east–west extension during at least mid- to Late Carboniferous time (e.g., Oversby 1983: *Geological Society of Australia, Abstracts,* 9, 112–113); a related transfer structure would be oriented at a high angle to them, as the TMIIB is. To the south of the TMIIB, late Palaeozoic granitoids with ignimbrite-dominated extrusives and cauldrons are exceedingly common. However, immediately north of the belt, similar late Palaeozoic intrusive and extrusive rocks are negligible in exposure, although evidently present sporadically beneath Mesozoic–Cainozoic cover (P. Wellman, AGSO, personal communication 1995). Granitoids and ignimbrites reappear only in real abundance in the Janet Ranges Volcanics, about 400 km north of the TMIIB. These observations are consistent with there being two contrasting tracts, of late Palaeozoic origin, immediately south and immediately north of the TMIIB. The contrasts (in abundances of appropriate igneous rocks, as responses to tectonism) between these tracts can fairly be ascribed to differing amounts, rates, and/or geometrical styles of extension. Juxtaposition of such contrasting tracts is, by definition, a characteristic of transfer structures.

The TMIIB contains by far the greatest spatial concentration (to the extent of being almost continuously coalesced) of late Palaeozoic felsic igneous rocks known or inferred in north Queensland south of the Janet Ranges Volcanics and Torres Strait area (northern Cape York Peninsula). This marked concentration of crustal melt material suggests that the belt was exceptionally 'leaky' — i.e., a magma conduit. The observation also implies that the belt extended to at least the (mid-crustal?) depths at which felsic melt was collecting into discrete, stock- and larger-size, magma chambers — possibly even to the lowermost crust and uppermost mantle (below).

The TMIIB probably underwent at least intermittent transtension (consistent with contemporaneous east–west extension external to the belt). This would have caused some degree of general stress relief at depth along its length, and probably led to the initiation of decompression melting of mantle material, and anatexis of lower crust by that material. Also, dilational jogs would have opened-up along any individual dislocations within the belt, particularly at brittle mid- to upper crustal levels. In consequence, magma focusing towards and into the belt would have been enhanced, as would more localised internal channelling. Permissive magma emplacement should have been as characteristic of the transfer structure as it was of more straightforwardly extensional tracts to the north and south; permissive emplacement is indeed confirmed by observations from exposed plutons (cf. Oversby et al. 1980: *op. cit.*), and by the presence of cauldron structures both exposed and geophysically inferred within the belt.

The southern edge of the TMIIB delimits north-younging extrusive stratigraphies and coalesced cauldrons of the major Newcastle Range volcano-tectonic structure; no extrusive rocks in cauldrons within the belt directly north of the Newcastle Range rocks and structures are spatially connected with, or unambiguously related to, them. This suggests that the TMIIB may have acted as a 'bulkhead', at least locally, resisting (and ponding?) north-propagating magmatism, as a fundamental deep transfer structure could be expected to do, almost by definition.

The Early Permian Agate Creek Volcanic Group and associated dykes in the Georgetown district have a trend essentially parallel to the TMIIB. Previously, this apparently distinctive association of rocks and trend was cited as evidence for an Early Permian northeast-to-southwest-directed minimum principal stress direction (Oversby 1983: *op. cit.*). Such an interpretation required a substantial degree of stress reorientation during latest Carboniferous and/or earliest Permian time, which seemed conceptually inappropriate. However, the stress reorientation required is radically reduced (if not eliminated) if the Agate Creek trend reflects a series of second-order accommodation structures related to the TMIIB. Similar west to west-northwest trends of fault zones crossing the Newcastle Range have already been interpreted in these terms (Oversby 1987: *op. cit.*).

The scale (particularly its considerable length), transverse orientation/transfer characteristic with respect to regional extension, and exceptional 'leakiness' of the TMIIB are consistent with the belt having been a local proto-rift formed in response to supra-regional late Palaeozoic membrane tectonics in a rapidly drifting south polar Gondwanaland (Oversby 1988: op. cit.; cf. Oxburgh & Turcotte, 1974: *Earth and Planetary Science Letters*, 22, 133-140, especially fig. 2). The Broken River Province (or Embayment) farther south may represent another one. The question of whether or not the TMIIB was the successor to some Siluro-Devonian or older structure remains to be evaluated further (P. Wellman, R. Blewett, AGSO, personal communications 1995).

That existence of the TMIIB has general implications for mineral deposit occurrences has already been noted (Wellman et al. 1994: *op. cit.*). Implicit in the transfer-structure hypothesis introduced briefly here is the conceptual possibility that mantle-derived mafic magmas may have have been present in greater-than-average (relative to the norm elsewhere in the late Palaeozoic of north Queensland) volumes in the TMIIB, and/or ascended to higher-than-average crustal levels within the confines of the belt. Conceptually again, specific commodity types and distributions within the belt may have been controlled by the influences which any such mantle-derived material could be expected to exert over interrelated petrogenetic and metallogenic processes. These potentially economic aspects of the TMIIB require fuller evaluation via specialist petrogenetic/metallogenic analysis and modelling.

For further information, contact Dr Brian Oversby (Division of Regional Geology & Minerals) at AGSO.

Airborne gamma-ray spectrometry as a tool for assessing relative landscape activity and weathering development of regolith, including soils

Introduction

Gamma-ray data can contribute significantly to an understanding of the weathering and geomorphic history of a region. AGSO is currently using it, together with traditional data sets (aerial photography and Landsat Thematic Mapper imagery), to assist in mapping regolith[1]. Data from airborne gamma-ray surveys in north Queensland (Wilford 1992: *AGSO Record* 1992/78) and central New South Wales (Bierwirth 1994: *Proceedings of the 7th Australasian Remote Sensing Conference*, 927–934) have been successfully applied to studies of the development and distribution of weathered materials, including their mineralogy, chemistry, and styles of weathering. They have also been used to map the distribution and trace the derivation of transported materials. The overview that follows draws on examples from a gamma-ray survey flown over the Ebagoola 1:250 000 Sheet area (N Qld).

[1] 'Regolith' herein refers to both soil and weathered material.

Factors effecting the gamma-ray response

Gamma-ray imagery can be regarded as a geochemical map showing the distribution of the radioelements — potassium (K), thorium (Th), and uranium (U) — in rocks and regolith. Most gamma-rays emanate from the top 30–45 cm of dry surface material (Grasty, 1976: 'Remote sensing for environmental science', *Springer-Verlag*, 257–276). Soils therefore have a major influence on the gamma-ray response. The gamma-ray response of soils commonly can be used to indicate the type of regolith below.

Gamma-rays emitted from the surface can be classified into primary and secondary sources. Primary sources relate to the geochemistry and mineralogy of the bedrock. Secondary sources relate to regolith (weathering products and processes) and radioelements in groundwater. During weathering, the distribution or relative concentration of these radioelements is modified from the initial bedrock source. K is geochemically mobile: it is soluble under most weathering conditions, wherein it is either lost in solution and/or absorbed onto clay minerals such as illite, montmorillonite, and to a lesser extent kaolinite. U is readily leached and released from soluble minerals under oxidising conditions, and precipitates in reducing conditions. Surface concentrations of U can be associated with resistate minerals such as zircon and monazite, or derived from radium-226 exsolved from groundwater. Th is geochemically immobile under most weathering conditions, and, since it is largely contained within resistate minerals, it tends to be concentrated in residual profiles. Both U and Th released during weathering are readily absorbed onto clay minerals, iron oxides, and organic matter in soils.

The modification of these radioelements during weathering and pedogenesis provides information on the regolith materials, and on geomorphic processes in the landscape which effect the distribution and development of the regolith.

Assessing relative geomorphic activity and weathering development

The development of a weathering profile depends on the balance between the rate of bedrock weathering and the rate at which weathered material is removed by denudational processes (Fig. 19).

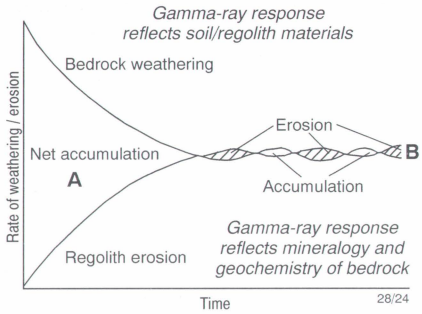

Fig. 19. Factors which effect the denudational balance in landscapes.

Regolith thickness at any one site will depend on the relative rates of accumulation and erosion: A — weathering rates higher than erosional rates, resulting in regolith development; B — weathering and erosional rates similar, resulting in thin permanently youthful regolith. In areas of erosion, gamma-ray responses are likely to reflect geochemistry and mineralogy of the bedrock, whereas in areas of accumulation the response is modified by pedogenesis. (Modified from Crozier 1986: 'Landslides: causes, consequences and environment'. *Croom Helm, London*, p. 138).

The most stable parts of the landscape are those where the weathering rate is high compared with the rate of erosion. Deep weathering profiles are, therefore, likely to develop in stable areas which have low relief and where rates of erosion are moderately low. The degree of regolith development can be determined by using well-established geochemical techniques based on mineral-weathering indices. These techniques ratio soluble mineral components (Ca, Na, K) to Al or resistant minerals, such as zircon, as an index of weathering. Similarly, airborne spectrometry can be used to assess regolith development because the loss of K during weathering, and the enrichment of Th and U associated with the accumulation of residual accessory minerals and oxides in the regolith, are detectable on gamma-ray images. The advantage of gamma-ray imagery over mineral-weathering studies is that regolith development can be mapped directly rather than extrapolated from spot geochemical sampling.

The relative mobilities of major mineral constituents released during weathering and their gamma-ray responses are shown in the sequence below.

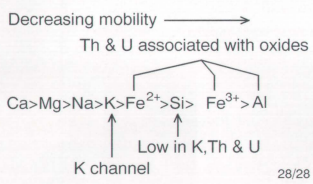

This sequence is generalised, and relative mobilities may change according to environmental conditions. Gamma-ray spectrometry can measure K directly, and silica, Fe, and Al indirectly.

In-situ regolith

Stable landscapes in the Ebagoola 1:250 000 Sheet area tend to be covered by either accumulations of Fe and Al oxides and resistate minerals, or residual quartz sands. Elevated Th and U values associated with surface concentrations of residual minerals (such as zircon and monazite) and Al/Fe oxides can be used to separate highly leached bauxitic regolith from more youthful weathering profiles developed on similar lithologies. Soil geochemistry shows that bauxitic sand and nodules are high in Th, U, and Zr, and low in K, Na, and Ca (Fig. 20a–b). However, not all high Th and U values in the gamma-ray image are associated with highly weathered regolith, because different bedrock types can give similar responses. The radioelement characteristics of the bedrock and weathered materials must be understood before the gamma-ray responses can be used to interpret the degree of regolith development.

Gamma-ray imagery over weathered granitic landforms distinguishes two main regolith types:

- completely weathered saprolite on gently sloping stable landforms; and
- thinner partly weathered saprolite on steeply sloping, actively eroding landforms.

In a completely weathered profile (Fig. 21), residual sand forms from deep chemical weathering, which results in the loss of soluble mineral constituents (K_2O, CaO, Na_2O) and the concentration of resistant quartz and accessory minerals (such as zircon and monazite; Fig. 20a–b) in the upper part. Residual quartz sand without accessory minerals is low in K, Th, and U, and appears black in gamma-ray images.

In contrast, thinner partly weathered profiles are distinguished by their higher K response. This response mainly reflects the presence of alkali-feldspars and mica from the partly weathered granite. Therefore, steeper hill slopes with high rates of erosion maintain thinner weathering profiles than stable landforms, and reflect correspondingly higher values in the K channel (Fig. 22). Conversely, where rates of weathering exceed rates of erosion, a decrease in K concentration occurs as K-bearing minerals are progressively leached from the weathering profile (Fig. 21). However, care should be taken when considering such relationships, because other regions, depending on their bedrock type and weathering history, may differ.

Transported regolith

The gamma-ray responses and geochemistry of sediments derived from similar bedrock provinces, but deposited in different environments, enable the relative depositional activity rates to be determined. Recently deposited channel sands sourced from mixed granitic and metamorphic provinces have high K, Th, and U values. The radioelement response from these sands closely reflects the chemistry of the bedrock from which they were derived. This suggests that erosion, transportation, and deposition of these sediments were moderately rapid, allowing insufficient time for weathering to modify the radioelement composition from the original bedrock source. Alternatively, the response may reflect winnowing of the sediments during transportation — removal of the fines, and polishing of the sand grains — leading to only fresh sands in the channel deposits.

In contrast, older alluvial-terrace and overbank sediments also derived from granitic and metamorphic rocks have lower K, but higher Th and U. These differences probably reflect:

- textural and compositional differences between the coarser channel sands and finer overbank sediments; and
- modification of the radioelements as a result of weathering and leaching.

Soil geochemistry (Fig. 20c–d) of the overbank and terrace sediments shows a lower concentration of readily soluble mineral constituents (CaO, NaO, K_2O), and a preferential increase in resistant minerals such as zircon, compared with channel sediments. This indicates a less active depositional regime in which there was sufficient time for weathering to modify the distribution and/or concentration of radioelements in the sediments before they were deposited. In the Ebagoola Sheet area, gamma-ray imagery has distinguished palaeochannel and former river channels according to the preferential loss of K and relative concentration of resistate minerals indicated by higher Th and U responses.

Conclusions

Gamma-ray imagery responds to different styles of in-situ weathering, which reflects underlying lithology, time, and geomorphic process. The imagery, therefore, has considerable potential for mapping the regolith. Relative depositional activity can be determined: active depositional environments with minimal weathering are distinguishable from less active depositional environments where pedogenetic processes have modified the surface radioelement chemistry. Once the gamma-ray response of the regolith and underlying bedrock are understood, the relative rates of regolith formation and removal can be mapped, and the denudational balance in the landscape assessed. In places the degree of regolith development can be determined. Interpretations of gamma-ray data for regolith are best made within major geological groups since relationships between gamma-ray response and weathering styles are often specific to particular bedrock types. In the Ebagoola Sheet area, mature highly weathered soils identified using gamma-ray imagery also

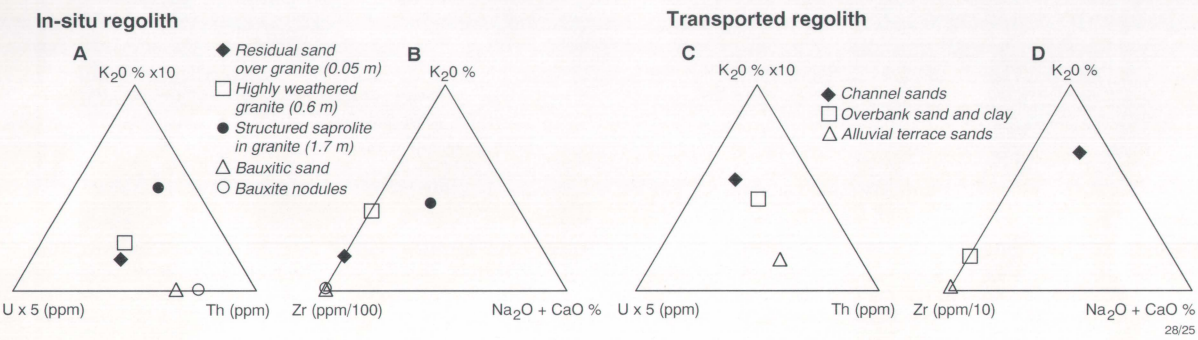

Fig. 20. Ternary diagrams of geochemical trends for K_2O, Th, U, Zr, and Na_2O + CaO based on preliminary regolith sampling: a, b — in-situ weathering profile on granite and bauxitic material; c, d — sediments derived from river channel, overbank, and alluvial terraces.

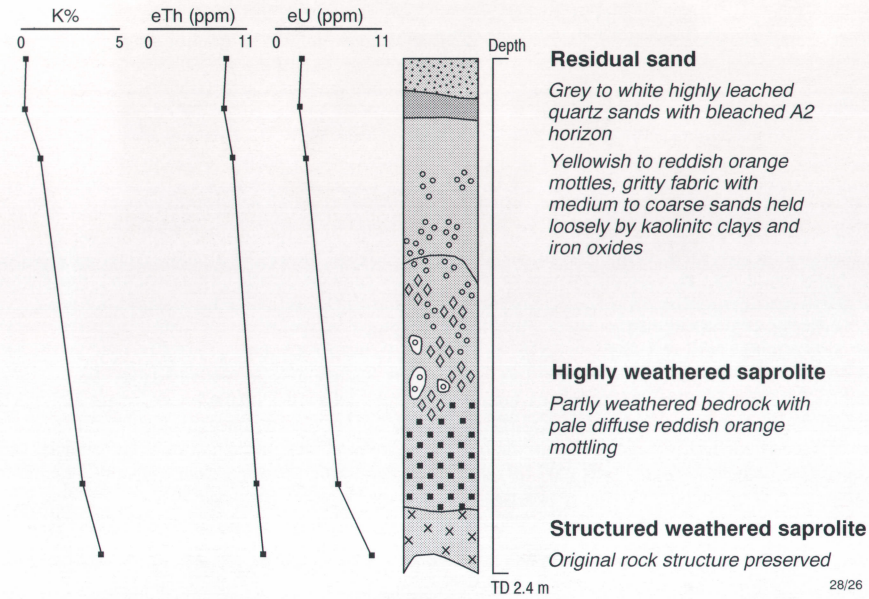

Fig. 21. Geochemical trends and the corresponding gamma-ray response down a completely weathered profile developed on granite in north Queensland (Ebagoola).
K%, and ppm equivalents of Th and U down the profile, were measured on a laboratory spectrometer.

have very low exchangeable cations and organic matter content. This highlights the potential application of airborne surveys for assessing and mapping nutrient status of certain soils.

For further information, contact John Wilford (Division of Regional Geology & Minerals) at AGSO.

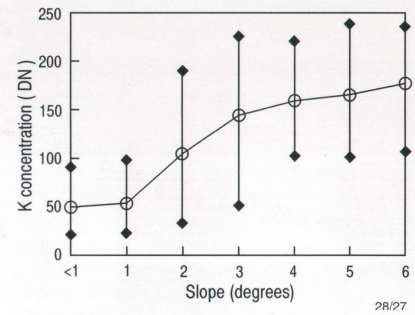

Fig. 22. Variation of imaged K concentration scaled from 0–255 (digital numbers; DN) against corresponding slopes derived from a digital elevation model.
The upper, lower, and mean K response within each slope class is indicated. As slopes increase, so does the rate of erosion, and the concentration of K.

Palaeomagnetism suggests mid-Carboniferous convergence between Greater Australia and Altaids

The mid-Carboniferous Kanimblan/Alice Springs Orogeny, which resulted in widespread and extensive deformation of Gondwanan Australia, coincided with the Variscan Orogeny, the result of northwest Gondwana's convergence with Laurussia to form Pangea, but only recently has a causal relationship between them been proposed (Veevers et al. 1994: *Basin Research*, 6, 141–157). The orogenic effects of Pangean convergence are generally thought to be restricted to the continents bordering the Atlantic. However, widespread 'Variscan' deformation also occurred throughout the extensive Altaid chains south of the Siberian craton (Zonenshain et al. 1990: *Geodynamics Series*, 21), and, according to palaeomagnetic evidence, reflects northward convergence between Baltica and the Siberian craton (Şengör et al. 1993: *Nature*, 364, 299–307). Further, new palaeomagnetic data obtained by AGSO from the Carboniferous ignimbrite succession of the Tamworth Belt, New England Orogen, suggest convergence of Greater Australia[1] with the Siberian craton. The new data indicate a hitherto unknown northward movement of Greater Australia through 40° of latitude during the Early Carboniferous,

[1] The present-day Australian continent plus fragments that have broken off the northern boundary and are now incorporated in southern Asia.

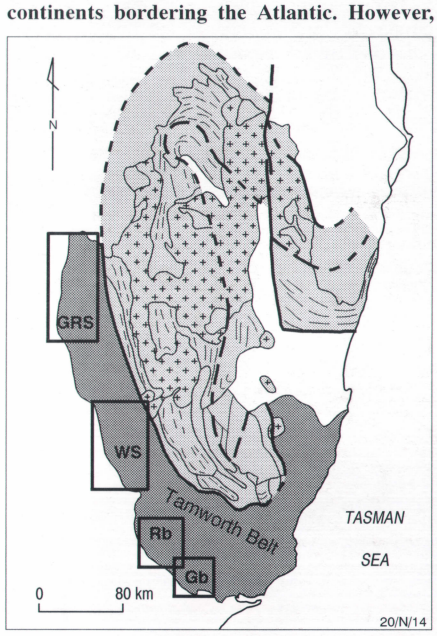

Fig. 23. Southern New England Fold Belt after Korsch & Harrington (1987: *Geodynamics Series* 19, 129–140) shows outlines of the four studied tectonic units in the Tamworth Belt. From north-to-south: Gravesend/Rocky Creek Syncline (GRS), Werrie Syncline (WS), Rouchel block (Rb), Gresford block (Gb).

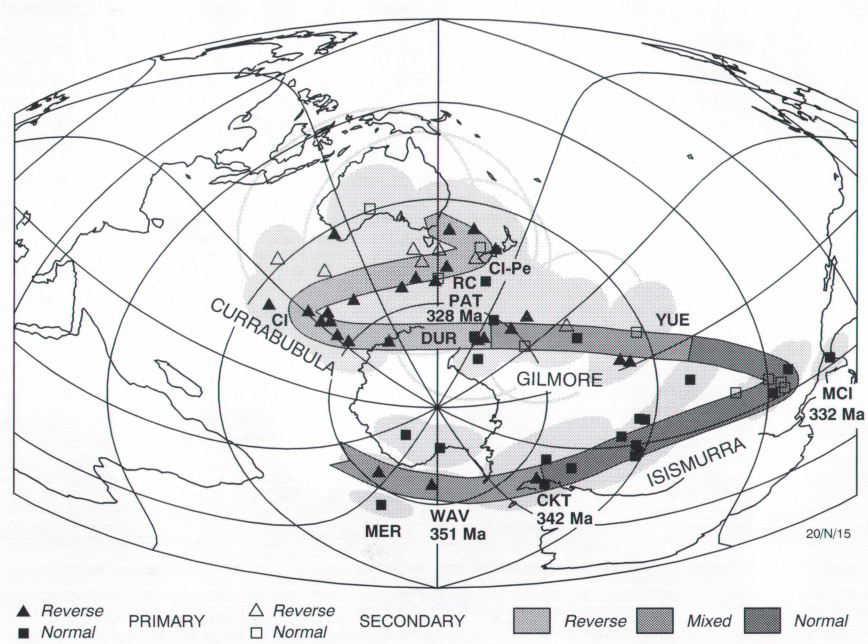

Fig. 24. Early Carboniferous-Late Permian APWP for New England/(neo-)cratonic Australia based on integration of APWP trajectories for the four studied tectonic blocks (Fig. 23).
MER = Merlewood Fm (Werrie Syncline); WAV = Waverley Fm (Rouchel block); CKT = Curra Keith Tongue (Rouchel block); MCI = Martins Creek Ignimbrite Member (Gresford and Rouchel blocks); YUE = Yuendoo Andesite Tuff (Gravesend/Rocky Creek Syncline); PAT = Paterson Volcanics (Gresford block); DUR = Mount Durham Tuff Member (Gresford block); RC = Rocky Creek Conglomerate (Gravesend/Rocky Creek Syncline; CI = Late Carboniferous; Pe = Early Permian..

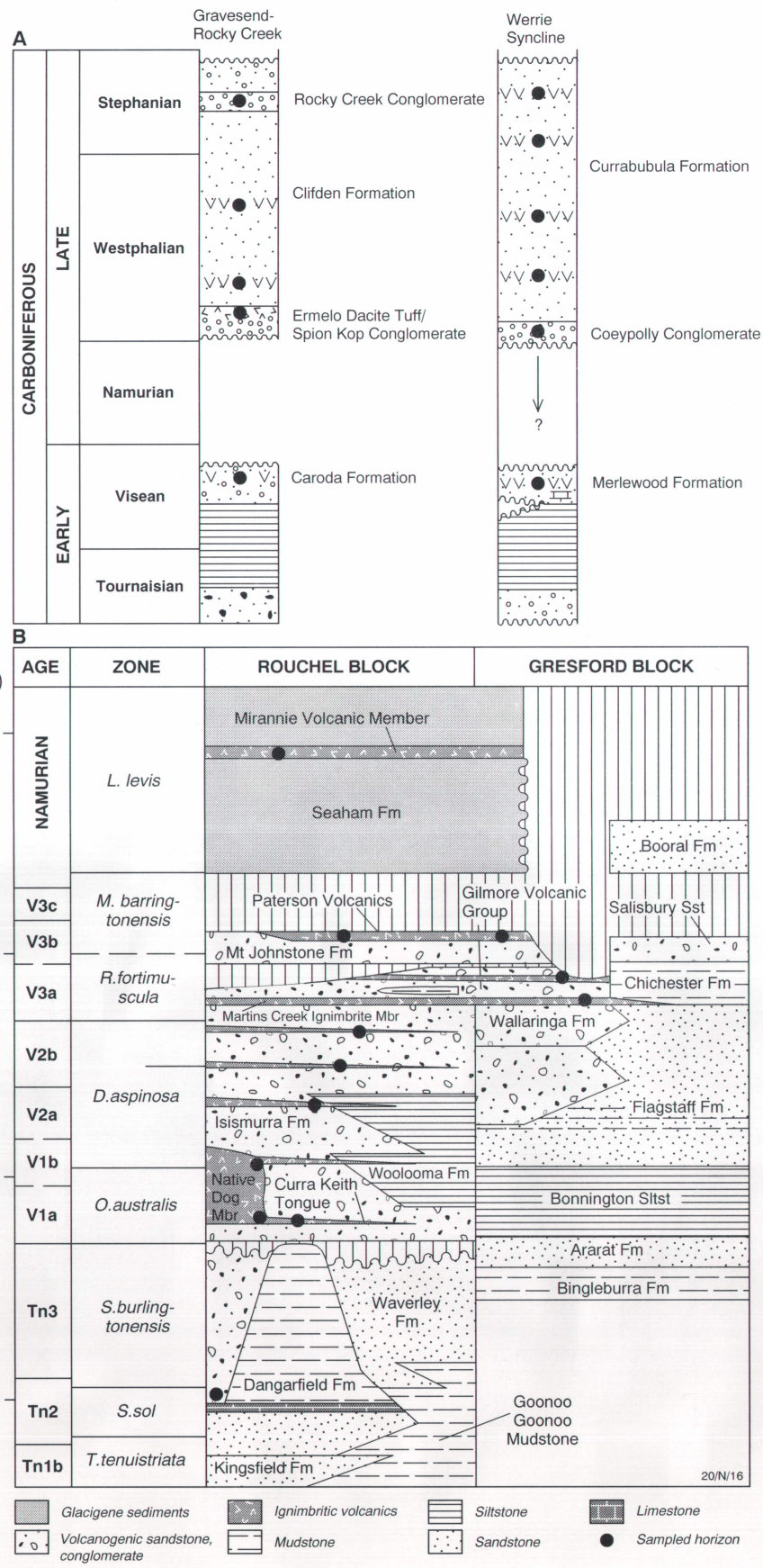

Fig. 25. Schematic stratigraphy of the sampled successions in the Gravesend/Rocky Creek and Werrie Synclines (A), and the Rouchel and Gresford blocks (B; after Roberts et al. in press).

before its well-documented Late Carboniferous large-scale southward movement to polar latitudes. Interpretation of this northward movement as involvement of Greater Australia in 'Variscan' deformation of the Altaids identifies the Kanimblan/Alice Springs Orogeny as a 'Variscan' Pangea-forming event.

The new palaeomagnetic data stem from an extensive collection of Carboniferous and Early Permian volcanics from the Tamworth Belt. Thermal demagnetisation data from about 500 pilot samples from four tectonic units in the belt (Gravesend/Rocky Creek Syncline, Werrie Syncline, Rouchel block, and Gresford block; Fig. 23) show no evidence for rotational deformation, and the pole track established for each of the four units has been combined into a Carboniferous–Early Permian apparent polar-wander path (APWP) for New England (Fig. 24). The APWP resembles a previously proposed polepath for (neo-)cratonic Australia (Klootwijk et al. 1993: *AGSO Record* 1993/36, fig. 12), but is characterised by a more extensive Early Carboniferous eastward swing. The extensive eastward swing probably represents a refinement of the APWP for Australia, rather than differential movement between New England and (neo-cratonic) Australia. Thus a recent provenance-linkage study (Flood & Aitchinson 1992: *Australian Journal of Earth Sciences*, 39, 539–544) has shown that New England had already accreted to (neo-)cratonic Australia by the latest Devonian. Such an early accretion is supported by the good agreement between the New England polepath and the (neo-)cratonic polepath for the earliest and Late Carboniferous.

The New England APWP (Fig. 24) reflects large-scale latitudinal and rotational movements that can be well-calibrated in age through AGSO's continuing program of SHRIMP (ion-microprobe) U–Pb dating of selected tuffs (e.g., Roberts et al. in press: *SEPM Special Publication*). A large eastward swing in the Early Carboniferous part of the APWP is well-defined by the volcanic succession of the Rouchel block (Fig. 25B) — the Waverley Formation and the Isismurra Formation in particular, and the Martins Creek Ignimbrite Member (332.3 ± 2.2 Ma) of the Isismurra Formation at the polepath's eastern apex. The initial part of the subsequent large-scale westward swing is poorly constrained by the Gilmore Volcanic Group of the Gresford block, but is better defined by the Yuendoo Andesite Tuff Member and West Lynne tuff (V2b) of the Caroda Formation in the Gravesend/Rocky Creek Syncline (Fig. 25A). The central part of the westward swing is well-defined by the Paterson Volcanics (328.5 ± 1.4 Ma)–Mount Durham Tuff Member (Seaham Formation) succession of the Gresford block. The younger end of the westward swing and also the subsequent eastward swing of smaller magnitude are well defined by the Upper Carboniferous Currabubula Formation in the Werrie Syncline, and by the Gravesend/Rocky Creek succession up to some tuffaceous intercalations in the Rocky Creek Conglomerate (Fig. 25A).

This extensive APWP is provocative in its radical difference from other proposed APWPs for Australia or Gondwana (e.g., Schmidt et al. 1994: *Exploration Geophysics*, 24, 257–262; Li et al. 1994: *Exploration Geophysics*, 24, 263–268). However, its robustness is supported by its distinctive polarity pattern. The polepath (Fig. 24) shows exclusive reverse polarity from the Mount Durham Tuff Member upwards. Results from the Isismurra Formation, however, reveal a previously unidentified normal-polarity interval of at least 10 Ma between extrusion of the Curra Keith Tongue (342.1 ± 3.2 Ma) of the Native Dog Member (Isismurra and Newtown Formations)

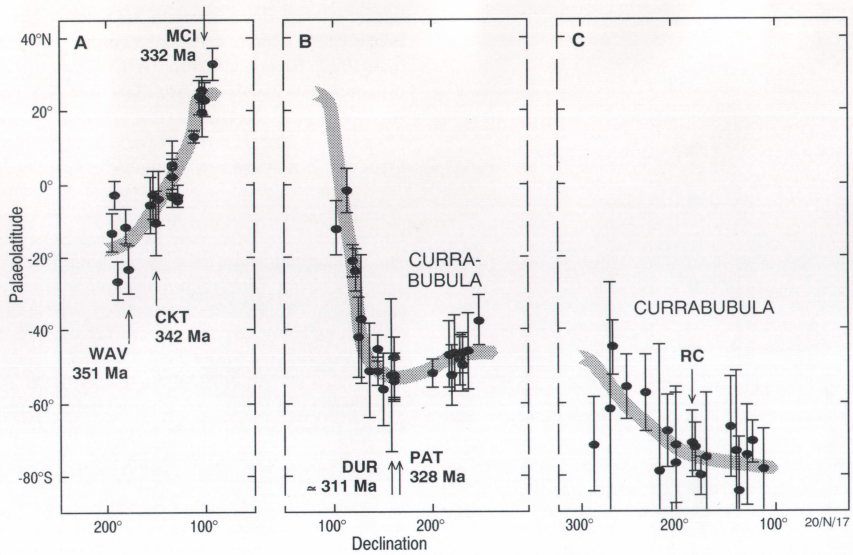

Fig. 26. Palaeolatitudinal evolution of New England/(neo-)cratonic Australia (Canberra reference) based on the pole positions detailed in Figure 24.

Palaeolatitudes are shown against declinations, as a relative age indicator, for the three successive APWP swings: Early Carboniferous eastwards (A), Late Carboniferous westwards (B) and Late Carboniferous–Early Permian eastwards (C). For abbreviations, see caption to Figure 24. Note that the palaeolatitudes shown are valid only for the Canberra reference locality, and do not represent palaeolatitudes for the continent as a whole; different parts of the continent may show palaeolatitude shifts that vary somewhat in magnitude from the pattern shown.

and the Martins Creek Ignimbrite Member. This normal-polarity interval is preceded and followed by mixed-polarity intervals.

The New England APWP (Fig. 24) indicates large and fast shifts in palaeolatitude (Fig. 26):

- rapid northward movement over about 40° of latitude, from about 15°S (Waverley Formation) to about 25°N (Martins Creek Ignimbrite Member; Fig. 26A) during the Early Carboniferous; and
- very fast and extensive southward movement to about latitude 50°S (Fig. 26B: Paterson Volcanics, Mount Durham Tuff Member) during the late Early to early Late Carboniferous, and ultimately reaching latitude 70°S by the Early Permian (Fig. 26C).

These new palaeomagnetic data, together with the SHRIMP ages, provide us with the means to determine rates of movement. Whereas the southward movement was expected (from well-established biostratigraphic indicators of a cooler climate), the preceding northward movement was not, and is provocative as it implies unrealistically high plate velocities for the succeeding southward movement — viz., about 75° in about 4 Ma (between extrusion of the Martins Creek Ignimbrite Member and the Paterson Volcanics). This problem may be due to the misinterpretation of the Martins Creek Ignimbrite Member as a normal-polarity interval (a reverse-polarity interpretation for this interval would imply a smaller southward movement over a longer timespan), or to unjustified equating of the magnetic and SHRIMP ages for the Paterson Volcanics. However, a reverse rather than normal polarity for the Martins Creek Ignimbrite Member is highly unlikely, as it would invoke erratic declination swings. Instead, the similar palaeolatitudes for the Paterson Volcanics and much younger Mount Durham Tuff Member (Figs. 26 and 27) make it more likely that the age assignment for the Paterson Volcanics magnetic result may be incorrect. Although this problem needs to be resolved, it does not fundamentally impinge on the interpretation of Early Carboniferous northward movement preceding Late Carboniferous southward movement for New England/(neo-)cratonic Australia.

Australian palaeolatitude data with reliable age-control show that the Carboniferous north–south excursion was followed by a Triassic–Jurassic excursion of smaller magnitude, and later, after fragmentation of Gondwana, by continuing Cretaceous–Cenozoic northward movement (Fig. 27). India's palaeolatitude data, not illustrated, show similar movement patterns (Klootwijk 1984: *Tectonophysics*, 105, 331–353; Klootwijk et al. 1992: *Geology*, 20, 395–398). The data for these two continents demonstrate northward excursions of Eastern Gondwana which coincided with the Variscan, Cimmerian, and Alpine phases of accretion of Gondwana fragments to the Altaid periphery of the Siberian craton. Thus Eastern Gondwana may have acted as a carrier for such fragments, in contrast to the prevalent notion (Şengör 1987: *Annual Review of Earth and Planetary Sciences*, 15, 213-244; Scotese *in* Klein & Beauchamp 1994: *Geological Society of America, Special Publication*, 288, 1–12) that these fragments constitute a rifted rim which crossed a wide-open Tethys while Eastern Gondwana remained at far southern latitudes. Support for such a carrier role for Eastern Gondwana can be found in the palaeolatitudinal pattern for the Tarim block, northwest China (Fig. 27), which is thought to have been formerly adjacent to northwestern Australia (Li et al. 1994: *Geological Society of Australia, Abstracts* 37, 248–249).

Both the Australian and Tarim data evince Early Carboniferous northward movement through about 40° of latitude. This similarity suggests that the Tarim block, and possibly other related eastern Asian blocks, moved as part of Eastern Gondwana's rim until mid-Carboniferous contact with the Altaids. Eastern Gondwana's movement then reversed southward as it separated from the Tarim block, which subsequently accreted on to the Altaids. Passive-margin extension, expected as a consequence of such a tectonic event, may be reflected in the mid-Carboniferous–Early Permian extension of Australia's North West Shelf (AGSO North West Shelf Study Group 1994: Proceedings of the West Australian Basins Symposium, *Petroleum Exploration Society of Australia, Perth*, 63–76), the Late Carboniferous–Permian climax of rifting of Indo-Pakistan's northwest margin (Pogue et al. 1992: *Tectonics*, 11, 871–883), the mid-Carboniferous onset of Panjal Traps volcanism in northwest India, and the Late Carboniferous initiation of Gondwana basins in eastern India and Western Australia.

Such an evolutionary scheme may offer a possible explanation for the well-established intermixing of the equatorial Cathaysian and northern Gondwanan floras in the Permo-Carboniferous; accordingly, the Cathaysian continents could be interpreted as fragments that broke off Gondwana's northern rim during the initial — low latitude — phase of Gondwana's southward movement. The scheme constrains final convergence of Gondwana with the Altaids to the late Visean (340–330 Ma) and implies a 'Variscan' rather than 'proto-Pacific' origin for the Kanimblan/Alice Springs Orogeny. It may thus offer an explanation for the well-established but poorly understood 100-km+ crustal shortening across the Amadeus Transverse Zone and the Tasman Fold Belt during the 340–320-Ma interval (Powell 1984: *Geology*,

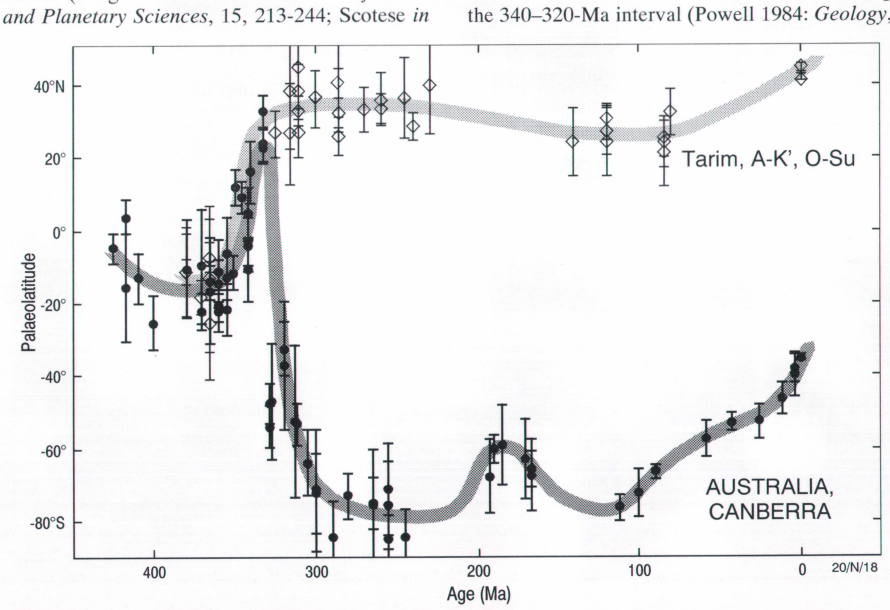

Fig. 27. Comparison of mid-Palaeozoic to Recent palaeolatitudinal control for Australia (Canberra reference, see caption to Fig. 26) and the wider Tarim block including the Junggar Basin and Kun Lun (A-K', O-Su reference).

12, 546–549). Constraints imposed by the east-trending declination pattern of part of the Tamworth Belt make it highly likely that the proposed movement pattern did affect the structural integrity of Gondwana.

For further information, contact Dr Chris Klootwijk (Division of Geophysical Observatories & Mapping) at AGSO.

Magnetic reference field models for 1995

The 1995 revision of IGRF

The International Geomagnetic Reference Field (IGRF) is a spherical harmonic representation of the Earth's main magnetic field of internal (core) origin. IGRF presently covers the interval from 1945 to 1995. Because of the secular change of the geomagnetic field, IGRF must be updated every 5 years. The latest, 1995, revision of IGRF is being coordinated by AGSO, and will comprise:

- a definitive main-field model for epoch 1990.0 (DGRF 1990);
- a provisional main-field model for epoch 1995.0 (IGRF 1995);
- a secular-variation model to cover the interval 1995.0 to 2000.0; and, possibly,
- DGRF models at 5-year intervals from 1900 to 1940.

Main-field models are truncated at spherical-harmonic degree and order 10; the secular-variation model at degree and order 8. DGRF 1990 will replace the now-obsolete IGRF 1990 provisional model. The new provisional model, IGRF 1995, will be replaced by a definitive model after 5 years.

Candidate models for the 1995 revision of IGRF have been submitted by NASA's Goddard Space Flight Center, the US Navy, the British Geological Survey, and the Russian Institute of Terrestrial Magnetism, Ionospheric and Radio Wave Propagation (IZMIRAN). The candidate models are currently being evaluated by agencies from around the world. A decision about which models to adopt for the 1995 revision of IGRF will be made by Working Group V-8 of the International Association of Geomagnetism and Aeronomy at the IUGG meeting in Boulder, Colorado next July. Release of the new coefficients can be expected in August or September 1995.

World Magnetic Model, epoch 1995.0 (WMM-95)

The US Navy and British Geological Survey recently released the spherical-harmonic coefficients (Table 1) for the 1995 update of the World Magnetic Model (WMM-95). The coefficients are made available free of charge, and are listed in Table 1. WMM-95 is truncated at degree and order 12, and therefore contains some of the long-wavelength crustal information that is omitted from IGRF. WMM-95 is used by the US Navy to produce the Epoch 1995.0 World Magnetic Charts, and is the basis of the magnetic direction-finding information that is included on many world navigational charts.

For further information, contact Dr Charles Barton (Division of Geophysical Observatories & Mapping) at AGSO.

Table 1. Spherical-harmonic (Gauss) coefficients of the US/UK World Magnetic Model for epoch 1995.0, WMM-95*

n	*m*	*gmn-MF (nT)*	*hmn-MF (nT)*	*gmn-SV (nT/y)*	*hmn-SV (nT/y)*
1	0	-29682.1	0.0	17.6	0.0
1	1	-1782.2	5315.6	13.2	-18.0
2	0	-2194.7	0.0	-13.7	0.0
2	1	3078.6	-2359.1	4.0	-14.6
2	2	1685.7	-418.6	-0.3	-7.2
3	0	1318.8	0.0	0.8	0.0
3	1	-2273.6	-261.1	-6.6	4.0
3	2	1246.9	301.0	-0.5	2.2
3	3	766.3	-416.5	-8.5	-12.6
4	0	940.0	0.0	1.2	0.0
4	1	782.9	259.4	1.1	1.3
4	2	290.9	-230.9	-6.8	1.0
4	3	-418.9	99.8	0.3	2.5
4	4	113.8	-306.1	-4.5	-1.2
5	0	-209.5	0.0	0.9	0.0
5	1	354.0	43.7	0.5	0.5
5	2	238.2	157.6	-1.4	1.5
5	3	-122.1	-150.1	-1.7	0.6
5	4	-162.8	-59.2	0.0	1.7
5	5	-23.3	104.4	2.1	0.6
6	0	68.5	0.0	0.4	0.0
6	1	65.6	-15.2	-0.3	0.7
6	2	64.1	74.3	0.3	-1.5
6	3	-169.1	69.4	2.1	-0.5
6	4	-0.5	-55.3	0.0	-0.7
6	5	16.5	3.0	-0.4	1.1
6	6	-91.0	33.3	-0.4	2.6
7	0	78.0	0.0	-0.3	0.0
7	1	-68.1	-76.1	-1.1	0.3
7	2	0.1	-24.5	-0.5	0.0
7	3	29.6	1.6	0.5	0.7
7	4	6.0	20.0	1.3	-0.6
7	5	8.7	16.5	0.1	0.1
7	6	9.2	-23.6	0.0	-0.6
7	7	-2.4	-6.8	-0.9	-0.4
8	0	24.7	0.0	0.1	0.0
8	1	3.4	14.9	0.0	0.4
8	2	-1.5	-19.5	0.4	-0.3
8	3	-9.6	6.3	0.3	0.1
8	4	-16.5	-20.4	-1.3	0.8
8	5	2.6	12.2	0.5	-0.1
8	6	3.6	7.0	0.4	-1.3
8	7	-4.9	-19.0	-0.9	-0.9
8	8	-8.5	-8.8	0.1	-1.1
9	0	2.9	0.0	0.0	0.0
9	1	7.5	-19.8	0.0	0.0
9	2	0.4	14.6	0.0	0.0
9	3	-10.3	10.9	0.0	0.0
9	4	9.7	-7.5	0.0	0.0
9	5	-2.3	-6.8	0.0	0.0
9	6	-2.4	9.3	0.0	0.0
9	7	6.8	7.7	0.0	0.0
9	8	-0.5	-8.1	0.0	0.0
9	9	-6.5	2.6	0.0	0.0
10	0	-2.9	0.0	0.0	0.0
10	1	-3.3	3.2	0.0	0.0
10	2	2.8	1.7	0.0	0.0
10	3	-4.3	2.9	0.0	0.0
10	4	-3.1	5.6	0.0	0.0
10	5	2.4	-3.4	0.0	0.0
10	6	2.8	-0.7	0.0	0.0
10	7	0.7	-2.9	0.0	0.0
10	8	4.1	2.3	0.0	0.0
10	9	3.6	-1.6	0.0	0.0
10	10	0.6	-6.6	0.0	0.0
11	0	1.7	0.0	0.0	0.0
11	1	-1.6	0.3	0.0	0.0
11	2	-3.6	1.0	0.0	0.0
11	3	1.2	-3.6	0.0	0.0
11	4	-0.6	-1.4	0.0	0.0
11	5	0.1	1.9	0.0	0.0
11	6	-0.7	0.2	0.0	0.0
11	7	-0.8	-1.3	0.0	0.0
11	8	1.3	-2.4	0.0	0.0
11	9	-0.3	-0.6	0.0	0.0
11	10	2.2	-2.2	0.0	0.0
11	11	4.2	1.3	0.0	0.0
12	0	-1.8	0.0	0.0	0.0
12	1	0.9	0.3	0.0	0.0
12	2	-0.1	1.4	0.0	0.0
12	3	-0.5	0.8	0.0	0.0
12	4	0.8	-3.0	0.0	0.0
12	5	0.2	0.7	0.0	0.0
12	6	0.5	0.5	0.0	0.0
12	7	0.4	-0.8	0.0	0.0
12	8	-0.4	0.6	0.0	0.0
12	9	0.3	0.1	0.0	0.0
12	10	0.2	-1.3	0.0	0.0
12	11	0.4	-0.4	0.0	0.0
12	12	0.6	0.9	0.0	0.0

* WMM-95 was produced by J.M. Quinn (US Navy) and S. Macmillan & D. Barraclough (British Geological Survey) on 5 December 1994.

Geochemistry as an aid to interpreting relationships in the Narwietooma Metamorphic Complex, Central Province of the Arunta Block, central Australia

Mapping Palaeoproterozoic Arunta basement in the Hermannsburg 1:250 000 Sheet area (a contribution to the Kimberley–Arunta National Geoscience Mapping Accord project, involving AGSO and the Northern Territory Geological Survey, NTGS) has laid the foundation for a moderately simple reconstruction of the geology of the Central Province, north of the Redbank Thrust Zone, where the stratigraphic units have been grouped into the Narwietooma Metamorphic Complex (Fig. 28; Warren & Shaw in preparation: 'Explanatory notes, Hermannsburg, SF53/13', 2nd edition, *NTGS, 1:250 000 Geological Map Series*). Geochemical data support conclusions made in field studies that units within the Complex interfinger and are composite, unified by metamorphism. Within the Complex, the Anburla Anorthosite and Mount Hay Granulite are probably comagmatic but unrelated to the Bunghara Metamorphics, which crop out along the northern edge of the MacDonnell Ranges (Fig. 28).

Units of the Narwietooma Metamorphic Complex in the south Central Province (Mount Hay Granulite, Bunghara Metamorphics) have a high proportion of meta-igneous rocks. The Mount Hay Granulite is mainly mafic, whereas the Bunghara Metamorphics range from intermediate to felsic and contain minor mafic rocks. The proportion of metasediments increases northward in units of the Complex.

A feature of the Narwietooma Metamorphic Complex is the abundance of meta-igneous rocks with intermediate SiO_2 contents (55–60 weight per cent, wpc; Fig. 29). Most Australian Proterozoic terranes (including most of the Arunta Block) show a distinctly bimodal distribution of SiO_2

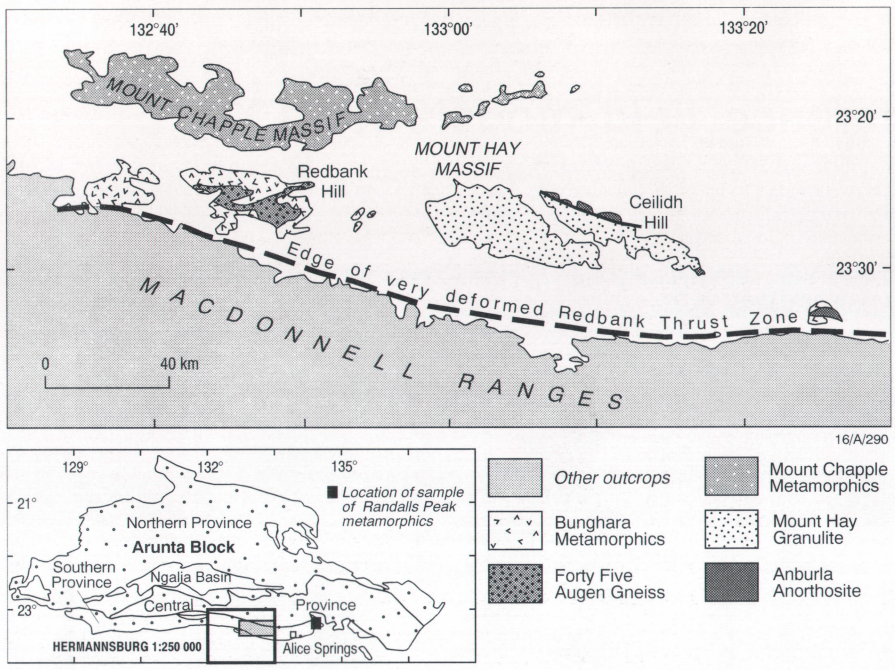

Fig. 28. Outcrops of the units of the Narwietooma Metamorphic Complex sampled in the Hermannsburg 1:250 000 Sheet area.

with a marked gap (e.g., Wyborn et al. 1987 *in* Pharaoh et al. (editors): *Geological Society of London, Special Publication* 33, 377–394). The Narwietooma Metamorphic Complex includes the Bunghara Igneous Suite (Warren & Shaw: *op. cit.*), which has 49–75 wpc SiO_2 and high TiO_2 and other incompatible elements (Figs. 29 and 30a). As defined, the Suite excludes mafic to intermediate rocks (including some cumulates) containing low TiO_2 and other incompatible elements. These may be of several ages.

Analyses show that some rocks from the Alice Springs 1:250 000 Sheet area — in particular, a sample of the Randalls Peak metamorphics, which has a SHRIMP (ion-microprobe) zircon age of 1771 ± 9 Ma (Zhao 1992: *PhD thesis, Australian National University*) — are also part of the Bunghara Igneous Suite. This probable age for the Suite is consistent with SHRIMP zircon ages in the range 1760–1750 Ma, which Black et al. (1992: *Australian Journal of Earth Sciences*, 39, 153–171) considered to be the igneous age for the syntectonic Forty Five Augen Gneiss intruding the Bunghara Metamorphics. The Mount Hay Granulite is affected by all phases of deformation (Watt 1992: *BMR Record* 1992/22), and so appears to be older than 1760 Ma (i.e., older than the Forty Five Augen Gneiss).

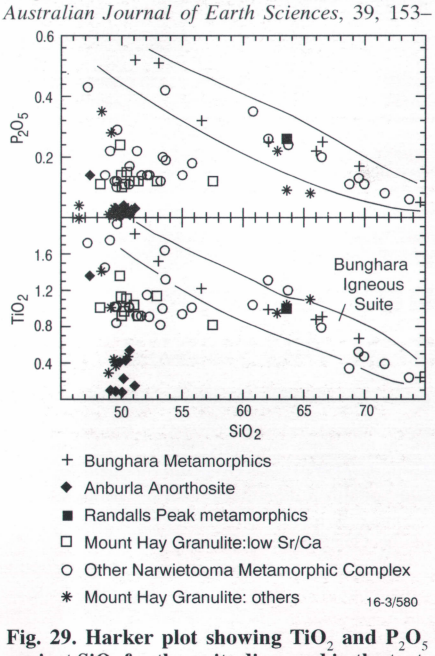

Fig. 29. Harker plot showing TiO_2 and P_2O_5 against SiO_2 for the units discussed in the text. The Bunghara Igneous Suite is outlined.

The Narwietooma Metamorphic Complex corresponds to a region of high magnetic response that continues northwest to the Mount Doreen 1:250 000 Sheet area, where it is masked by the non-magnetic Lander Rock beds. As the Lander Rock beds are intruded by granite dated at 1880 Ma (Young et al. 1992: abstract *in* 'The application of geochronology to field-related geological problems', *Geological Society of Australia SGGMP Workshop, Alice Springs*), the Narwietooma Metamorphic Complex, which appears to underlie them, must be older than 1880 Ma. Warren & Shaw (*op. cit.*) explained the apparent conflict by suggesting that the Narwietooma Metamorphic Complex includes two components. The older one might have formed ca 1880 Ma in a back-arc region in the Central Arunta Province between a clastic wedge (Lander Rock beds), and an arc-like region in the southeast Arunta Block which is now represented by rocks intruded by the Atnarpa Igneous Complex (dated at 1880 Ma by Zhao et al. 1992: *Precambrian Research*, 227–253). Some of the mafic rocks in the Narwietooma Metamorphic Complex have geochemical features (Fig. 30b) indicative of a back-arc environment. Alternatively, the Narwietooma Metamorphic Complex may include unrecognised Archaean basement. Both the Mount Hay Granulite and the Forty Five Augen Gneiss have Sm–Nd model ages (ca 2300 Ma; Black et al. 1984: *Australian Journal of Earth Sciences*, 31, 49–60; Sun et al. in press: *Precambrian Research*) that indicate a substantial Archaean component.

The Anburla Anorthosite forms three outcrops: one faulted into the Bunghara Metamorphics, and two abutting the Mount Hay Granulite, probably also in faulted contact. In addition, in Ceilidh Hill, the Mount Hay Granulite contains numerous thin sheets, from a few metres to about 100 m thick, of plagioclase-rich rocks. The Anorthosite includes minor coarse metagabbronorite. Warren & Shaw (*op. cit.*) postulated that the Anburla Anorthosite and Mount Hay Granulite are comagmatic: the Anorthosite first crystallised (perhaps as rafts) in a parent magma chamber, and the residual melt formed the mafic protoliths of the Mount Hay Granulite.

Many samples of Mount Hay Granulite have lower Sr, CaO, and Sr/Ca, but higher Ba than the Anburla Anorthosite. This set of low Sr/Ca samples from the Mount Hay Granulite is mafic (48–52 wpc SiO_2), and has spidergrams with distinct Sr-depletion and higher TiO_2, P_2O_5, and REE (Fig. 30c), consistent with residue after plagioclase extraction. Fe/Mg exchange was maintained between interstitial liquid in the cumulates and the residual melt, resulting in overlap of *mg* (100MgO/[MgO + total FeO]) between the Anorthosite and the Granulite. The data are consistent with the hypothesis that the Anburla Anorthosite and at least part of the Mount Hay Granulite are comagmatic. If so, then the Anburla Anorthosite should be relegated to member status within the Mount Hay Granulite, rather than being treated as a separate intrusion into the Narwietooma Metamorphic Complex. Other units in the Narwietooma Metamorphic Complex, mainly the Mount Chapple Metamorphics, contain rocks similar to the low Sr/Ca Mount Hay Granulite, thus providing geochemical evidence that the Mount Hay Granulite and the Mount Chapple

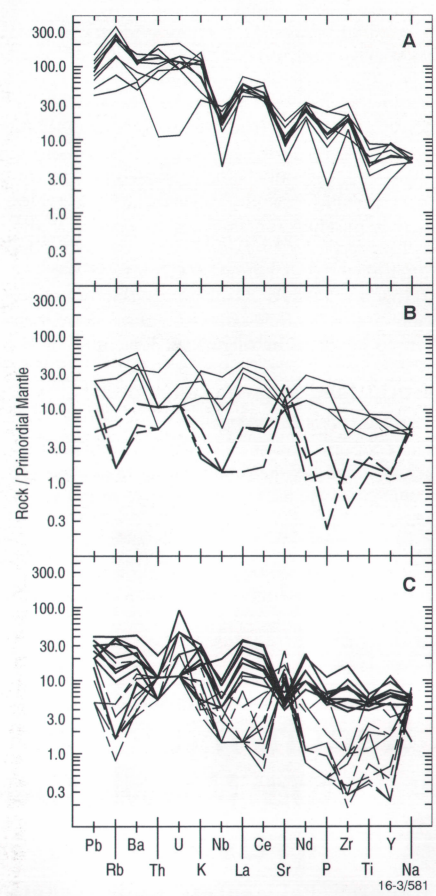

Fig. 30. Multielement plots (spidergrams) for (a) the Bunghara Metamorphics and Randalls Peak metamorphics, illustrating the chemical characteristics of the Bunghara Igneous Suite; (b) selected mafic granulites from the Narwietooma Metamorphic Complex, showing the presence of both back-arc (broken lines) and intracontinental (solid lines) types; and (c) the Mount Hay Granulite with low Sr/Ca (solid lines), and the Anburla Anorthosite (broken lines).

Metamorphics interfinger. (The Mount Chapple Metamorphics also contain rocks of the Bunghara Igneous Suite; Warren & Shaw *op. cit.*)

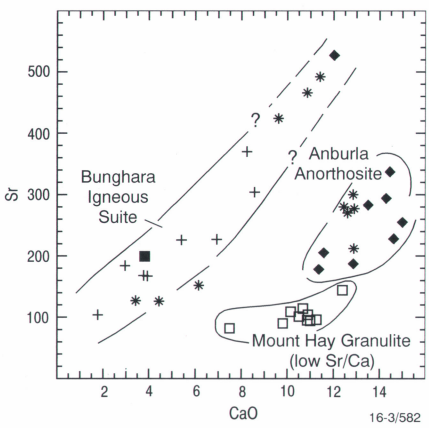

Fig. 31. Plot of Sr against Ca for selected units in the Narwietooma Metamorphic Complex. The position of the low Sr/Ca subset of the Mount Hay Granulite relative to the Anburla Anorthosite is consistent with plagioclase extraction. The possible extension of the Bunghara Igneous Suite to include samples from the southern Ceilidh Hill is indicated. (Symbols as in Fig. 29.)

Continued from p. 20

late Archaean crust took place in the Palaeoproterozoic, as evidenced by new zircon growth and zircon selvedges formed at ~1970 and 1880 Ma in the leucogranite.

The metasediments in the Browns Range Dome include arkose with detrital zircons ranging in age from 2470 Ma to 3460 Ma. Several clear age groups are apparent in this range. The youngest group has an age of 2507 ± 22 Ma, representing a maximum depositional age for the arkose sequence. Groups at 3050 ± 30, 3140 ± 10, and ~3410 Ma mimic ages for inherited zircon in the nearby grey gneiss and in the leucogranite that intrudes the arkose. There is an additional detrital population at ~3270 Ma.

Detrital zircons with similar ages, and some dated at 3600 Ma, are also present in sandstone of the Saunders Creek Formation, at the base of the Palaeoproterozoic Halls Creek Group in the East Kimberley. These zircon data reinforce the view that rocks as old as early–mid-Archaean might be components of the unexposed lower crust of northern Australia.

Conclusions

The new zircon U–Pb ages, together with Nd-isotope model ages and whole-rock geochemistry, demonstrate the existence in The Granites–Tanami region of largely concealed late Archaean complexes. The exposed Archaean rocks are vestiges of basement terranes on which subsequent Palaeoproterozoic basins were developed. As such, the 2500-Ma-old terranes are analogues of the Rum Jungle and Nanambu Complexes in the Pine Creek region, and may be prospective for the products of similar styles of economic mineralisation, particularly unconformity related Au–U.

For further information, contact Drs Rod Page, Shen-su Sun, or David Blake (Division of Regional Geology & Minerals, AGSO); Mr David Edgecombe (Dominion Mining Ltd); or Mr David Pearcey (PNC Exploration Australia Pty Ltd).

Distinct trends in Figure 31 show that a genetic relationship between the Bunghara Igneous Suite and the low Sr/Ca Mount Hay Granulite–Anburla Anorthosite is quite unlikely. Neither the Anburla Anorthosite–Mount Hay Granulite parent magma nor the residue after the crystallisation of the Anburla Anorthosite could be parent magma to the Suite. However, three samples of Mount Hay Granulite, and one assigned to the Anburla Anorthosite, from the thinly layered plagioclase-rich Mount Hay Granulite in the southern part of Ceilidh Hill are higher in Sr, and may be potential restite from and/or parental magma to the Suite, whose spidergrams (Fig. 30a) show Sr depletion (plagioclase fractionation).

Mapping of the Narwietooma Metamorphic Complex to date has been essentially at the reconnaissance level. The geochemical study has helped show that it is polygenetic, and indicated aspects of the geology that should be investigated in future studies.

For furthur information, contact Dr Gladys Warren (Division of Regional Geology & Minerals) at AGSO.

Chemical oceanography of Port Phillip Bay

AGSO and the Victorian Fisheries Research Institute (VFRI) applied the continuous geochemical tracer (CGT) technology aboard RV *Rig Seismic* to record continuous profiles of sea-water nutrients — nitrate (+ nitrite), ammonium, phosphate, and silicate — and hydrocarbons between Victoria Dock (in the Yarra River) and the entrance to Port Phillip Bay during April 1994. As a result, sea-water-nutrient data were measured and recorded at intervals of every 10 s (or, for a ship speed of about 6 knots, at distances over the sea-floor of about 25 m), and integrated with hydrographic data. About 100 km of continuously profiled data were collected in a 10-hour period.

To identify key reactions of nutrients in sea water, the data were normalised to salinity, which — being a conservative tracer — is unreactive in sea water. Simple chemical–oceanographic end-member mixing diagrams (Fig. 32; the two end-members being the Yarra River estuary water at Victoria Dock, and the Bass Strait source water) show that the highest nutrient concentrations were measured in the Yarra River estuary, and lowest concentrations in Bass Strait. If simple mixing controlled the property-distribution plots (Fig. 32), then all data would fall along the mixing line between the end-members. However, the data for nitrogen show that both ammonium and nitrate fall below the mixing line, a result that indicates loss of nitrogen from the water column — probably via uptake into diatoms, the main phytoplankton species in the bay. This process, known as primary production, results in the formation of particulate organic matter, most of which sinks quickly to the sea-floor. The data suggest that nitrogen is limiting for the production of organic matter, which agrees with earlier observations by VFRI.

Similarly, silicate data fall below the simple mixing line, even though silicate is not depleted entirely in the water column, and some silicate is exported to Bass Strait. Phosphate data show an apparent conservative behaviour: the data shown in Figure 32 suggest that the amount of phosphorus incorporated into particulate organic matter is small compared with the large pool of dissolved phosphate in the water column.

The capability of the CGT technique to measure the concentration of sea-water nutrients reflects an expansion by AGSO in the development of this technology, which was previously used to detect discharge from ocean outfalls off Sydney (*AGSO Research Newsletter*, 16, 23–24). The technique will now also detect and trace other parameters important in marine environmental geochemistry — notably petroleum hydrocarbons (BTEX: benzene, toluene, ethylbenzene, and the xylenes), sea-water nutrients, and hydrographic data (temperature, salinity, dissolved oxygen, turbidity, and percentage light transmission). In addition, sea-water samples can be collected in transit in the ship laboratory for other shore-based analyses of such components as heavy metals, industrial and agricultural chemicals, and sewage biomarkers.

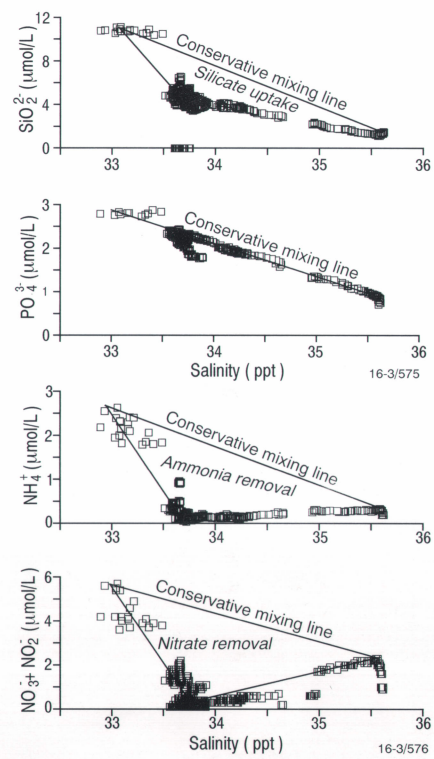

Fig. 32. Cross-plots of salinity v. (from top to bottom) silicate, phosphate, ammonium, and nitrate + nitrite for the pilot survey in Port Phillip Bay.

The outcome of this expansion has been to provide a new technique for rapidly collecting copious sea-water data which are amenable to large-scale contouring, and — for Australia's coastal environments — a tool for presenting synoptic perspectives of nutrient and other chemical distributions in large water masses. When combined with simple end-member mixing diagrams, the technique helps to identify both point and non-point sources of discharge, and the locations of key processes (both removal and inputs) which control the nutrient distributions.

For more information, contact Dr David Heggie (Division of Environmental Geoscience & Groundwater) at AGSO.

Geochronology of an exposed late Archaean basement terrane in The Granites–Tanami region

In only a few parts of the North Australian Craton is late Archaean (2500–2600 Ma) basement seen to underlie Palaeoproterozoic sequences. The two best known examples are the Rum Jungle and Nanambu Complexes, both in the Pine Creek Inlier. Though the existence of Archaean basement beneath and between most of the Palaeoproterozoic rocks of the craton remains conjectural, Nd-isotopic model ages, and U–Pb ages of inherited zircon components in igneous rocks and detrital zircon components in sedimentary rocks, provide indirect evidence for it.

Two late Archaean granitic gneiss terranes, close analogues of the Rum Jungle and Nanambu Complexes, have now been identified in The Granites–Tanami region — currently being investigated, in collaboration with Dominion Mining Ltd and PNC Exploration (Australia) Pty Ltd, as part of the Kimberley–Arunta National Geoscience Mapping Accord project. The two terranes are the Billabong complex (informal name) east of The Granites and the Browns Range Dome northwest of Tanami (Fig. 33).

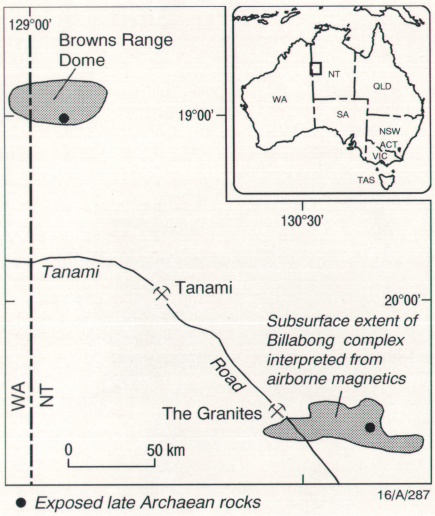

Fig. 33. Locality map, The Granites–Tanami region.

Geological relationships

Billabong complex. Situated in the southwest Mount Solitaire 1:250 000 Sheet area, this complex corresponds to a distinctive 'mottled' magnetic pattern on imaged aeromagnetic data that AGSO acquired from The Granites–Tanami region in 1993; this pattern contrasts with linear magnetic patterns of adjacent Palaeoproterozoic Mount Charles beds. Except for a few small exposures of banded granitic (quartz–feldspar–biotite) gneiss, it is completely covered by Cainozoic sand. The metamorphic grade of the granitic gneiss is much higher than that of exposed metasediments of the Mount Charles beds nearby.

Browns Range Dome. This east–west-elongated dome straddles the Northern Territory–Western Australia border at around latitude 19°S. It is outlined by ridges of outwardly dipping Gardiner Sandstone, the basal formation of the unmetamorphosed Mesoproterozoic or Palaeoproterozoic Birrindudu Group. Scattered exposures of basement gneiss, granite, and arkosic and conglomeratic metasediments occur in the central part of the dome, but most of this area is concealed by Cainozoic sediments. At one locality in the southern part of the dome (Fig. 33) leucocratic biotite granite encloses a block of grey quartz-rich biotite gneiss at least 20 m long. Drilling undertaken by PNC Exploration shows the grey gneiss to be more extensive in the subsurface. Both the granite and grey gneiss are cut by pegmatite veins. Similar granite and pegmatite intrude deformed arkosic metasediments exposed nearby.

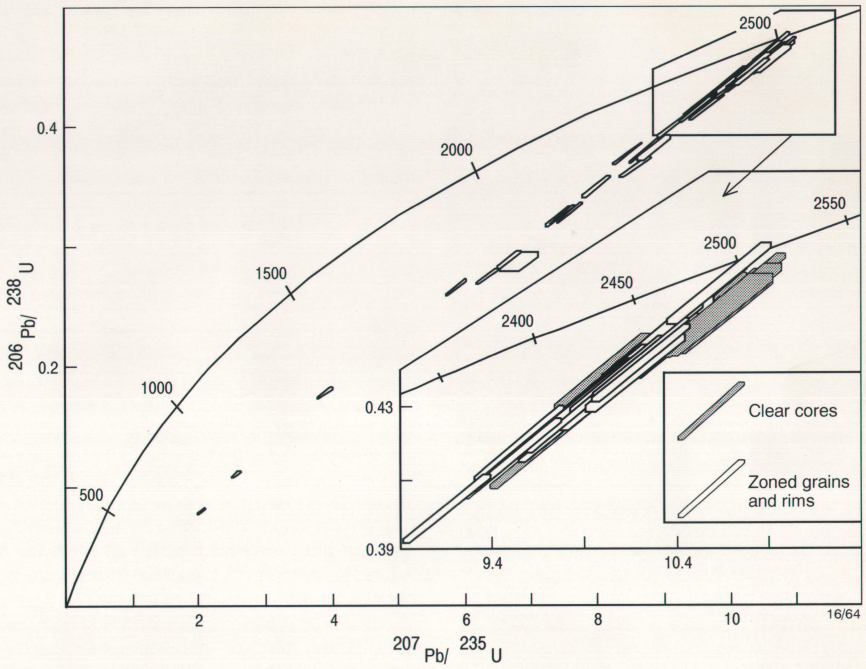

Fig. 34. Concordia plot of zircon U–Pb SHRIMP data from a late Archaean granitic gneiss in the Billabong complex, The Granites–Tanami region. Error boxes show 1-sigma analytical uncertainties, and quoted age errors are 95% confidence limits.

Geochemistry and Sm–Nd-isotope systematics of the basement rocks

The Billabong complex granitic gneiss and the Browns Range Dome granite are geochemically more akin to some late Archaean I-type granites in the Nanambu Complex of the Pine Creek Inlier than to typical Palaeoproterozoic granites of northern Australia. In addition, they have older Nd T_{DM} model ages (indicating average crustal residence time) of 2516 to 3297 Ma, compared with 2200 to 2500 Ma ages commonly found for Palaeoproterozoic granites and metasediments of northern Australia. Meta-arkose from the Browns Range Dome also has a moderately old Nd T_{DM} model age (2965 Ma). These data indicate a major contribution from Archaean source rocks. The oldest Nd T_{DM} model age determined (3297 Ma) was for the grey gneiss enclave in the Browns Range Dome.

New geochronological data

Billabong complex. The U–Pb data from SHRIMP analyses of zircon reveal a complex late Archaean history for the exposed banded granitic gneiss (Fig. 34). Two main populations of inherited zircon are evident, one at about 2550 Ma and the other at 2530 ± 4 Ma. These are interpreted as relics of zircon xenocrysts from lower crustal regions. The remaining zircon grains and rims surrounding inherited grains, although complexly zoned, provide a consistent age of 2514 ± 3 Ma. This is the best estimate for the igneous age of the granitic gneiss, which is therefore part of a crustal domain formed in the late Archaean.

Browns Range Dome. The zircon U-Pb data for the grey gneiss and leucogranite are again complex, and reflect a protracted Archaean history for the source rocks. Evidence of crustal formation at ~3400, 3140, 3040, and 2700 Ma is given by inherited zircon components in the two rocks. Most of the zircon data for the leucogranite form a discordant spectrum between 2600 and 2135 Ma old, including one group at 2510 ± 22 Ma. This age is indistinguishable from 2504 ± 4 Ma, the age of the main zircon population in the grey gneiss. Major recycling and metamorphism of this

Continued on p. 19

The *AGSO Research Newsletter* is published twice a year, in May and November. For further information please contact AGSO Marketing & Information Section, tel. (06) 249 9623, fax 249 9982. Correspondence relating to the *AGSO Research Newsletter* should be addressed to Geoff Bladon, Editor, *AGSO Research Newsletter*, Australian Geological Survey Organisation, GPO Box 378, Canberra ACT 2601; tel. (06) 249 9111, extn 9249; fax (06) 249 9987.
 ISSN 1039-091X A52930 PP255003/00266